Dark Universe 1 (2012) 194–217

Contents lists available at SciVerse ScienceDirect

Dark Universe

journal homepage: www.elsevier.com/locate/agee

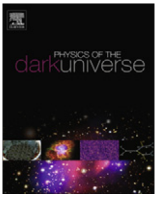

Gamma ray signals from dark matter: Concepts, status and prospects

Torsten Bringmann [a,*], Christoph Weniger [b]

[a] II. Institute for Theoretical Physics, University of Hamburg, Luruper Chaussee 149, DE-22761 Hamburg, Germany
[b] Max-Planck-Institut für Physik, Föhringer Ring 6, 80805 Munich, Germany

ARTICLE INFO

ABSTRACT

Weakly interacting massive particles (WIMPs) remain a prime candidate for the cosmological dark matter (DM), even in the absence of current collider signals that would unambiguously point to new physics below the TeV scale. The self-annihilation of these particles in astronomical targets may leave observable imprints in cosmic rays of various kinds. In this review, we focus on gamma rays which we argue to play a pronounced role among the various possible messengers. We discuss the most promising spectral and spatial signatures to look for, give an update on the current state of gamma-ray searches for DM and an outlook concerning future prospects. We also assess in some detail the implications of a potential signal identification for particle DM models as well as for our understanding of structure formation. Special emphasis is put on the possible evidence for a 130 GeV line-like signal that we recently identified in the data of the Fermi gamma-ray space telescope.

1. Introduction

Evidence for a sizable non-baryonic and cold dark matter (DM) component in the universe derives from an impressive range of unrelated cosmological observations [1], covering distance scales from tens of kpc to several Gpc and leaving very little room for alternative explanations. On cosmological scales, DM contributes a fraction of $\Omega_\chi = 0.229 \pm 0.015$ to the total energy density of the universe [2]. Weakly interacting massive particles (WIMPs) provide a theoretically particularly appealing class of candidates for the so far obscure nature of DM [3], with the lightest supersymmetric neutralino often taken as a useful template for such a WIMP. It is often argued that the thermal production of

* Corresponding author.
E-mail addresses: torsten.bringmann@desy.de (T. Bringmann), weniger@mpp.mpg.de (C. Weniger).

2212-6864
http://dx.doi.org/10.1016/j.dark.2012.10.005

Table 1
Rough comparison of basic telescope characteristics relevant for indirect DM searches with gamma rays, for a selection of typical space- and ground-based experiments that are currently operating, shortly upcoming or planned for the future. The quoted sensitivity is for point sources at the 5σ level, after 1 year (50 hrs) of space- (ground-) based observations and assuming typical backgrounds. Where applicable, numbers refer to photon energies at or above $E \simeq 100$ GeV (1 TeV). The angular resolution $\Delta\theta$ denotes the 68% containment radius. More details in Refs. [16] (Fermi-LAT), [17] (AMS-02), [18] (GAMMA-400), [19] (MAGIC), [20] (HESS-II) and [21] (CTA).

	Time of operation	*E*-range [GeV]	$A_{\rm eff}\,[{\rm m}^2]$	Sens. $[10^8\ {\rm m}^2\ {\rm s}]^{-1}$	$\Delta E/E$ [%]	F.O.V. [sr]	$\Delta\theta$ [°]
Fermi-LAT	2008–2018*	0.2–300	0.8	200	11	2.4	0.2
AMS-02/Ecal	2011–2021*	10–1000	0.2	1000	3	0.4	1.0
AMS-02/Trk	2011–2021*	1–300	0.06	1000	15	1.5	0.02
GAMMA-400	2018*–...	0.1–3000	0.4	100	1	1.2	0.02 (0.006)
MAGIC	2009–...	$\gtrsim 50$	2×10^4 (7×10^4)	10 (0.2)	20 (16)	0.003	0.17 (0.08)
HESS-II	2012–...	$\gtrsim 30$	4×10^3 (10^5)	4 (0.1)	15 (15)	0.003	0.13 (0.07)
CTA	2018*–...	$\gtrsim 20$	5×10^4 (10^6)	1 (0.02)	20 (10)	>0.006	0.1 (0.06)

* Planned.

WIMPs in the early universe generically leads to a relic density that coincides with the observed order of magnitude of Ω_χ, though this rests on the assumption of a standard cosmological expansion history and there exist well-motivated particle physics scenarios that predict alternative production mechanisms for WIMP DM [4]. While the LHC non-observation of new particles below the TeV scale (apart, possibly, from the Higgs boson) has already prompted doubts whether the WIMP DM scenario is still our best bet [5], it must be stressed that electroweak low-energy observables ($g-2$ in particular) do favor new physics contributions not too far above 100 GeV [6]. While this tension starts to considerably disfavor very constrained models of, e.g., supersymmetry [7], it may simply be an indication that the new physics sector which the WIMP belongs to appears at a much smaller mass scale than any new colored sector.

Attempts to identify WIMP DM can be classified into collider searches for missing transverse energy, direct searches for the recoil of WIMPs off the nuclei of terrestrial detectors and indirect methods that aim at spotting the products of WIMP self-annihilation. Among possible messengers for such indirect searches, *gamma rays*play a pronounced role as they propagate essentially unperturbed through the galaxy and therefore directly point to their sources, leading to distinctive *spatial signatures*; an even more important aspect, as we will see, is the appearance of pronounced *spectral signatures*. This prime role of gamma rays provides our motivation for an updated and dedicated review on these messengers, which we hope will prove useful and complementary to existing general reviews on indirect DM searches [8]. Indeed, the recent indication for a DM signature in gamma-ray observations of the Galactic center (GC) [9,10] makes such a review extremely timely, and we therefore dedicate a considerable part of it to discuss in great detail both the status of the potential signal and its implications.

Gamma rays can either be observed directly from space or, via the showers of secondary particles they trigger in the atmosphere, indirectly with ground-based experiments. The former option necessarily implies rather small effective areas and an upper bound on the photon energy that can reliably be resolved, but allows for a large field of view and the observation of gamma rays at comparably small energies. Particularly promising instruments for the latter option are imaging Air Cherenkov Telescopes (IACTs) that detect the Cherenkov light emitted by the shower particles and use efficient image reconstruction algorithms to determine the characteristics of the primary photon. These instruments have a limited field of view and a lower energy threshold set by the need of discriminating photons from the background of primary muons and hadronic cosmic rays; their extremely large effective area and rather small field of view make them ideal for pointed observations. In Table 1, we pick typical examples for space- and ground-based experiments that are currently operating or planned for the future and compare some basic telescope characteristics that are particularly relevant for DM searches. Experiments that fall into the same broad categories but are not listed explicitly in the table include for example AGILE [11] and VERITAS [12], as well as the future CALET [13] and DAMPE [14,15].

We stress that the numbers in Table 1 are intended to provide a convenient order-of-magnitude comparison of instrumental characteristics; they should *not*be used as the basis of detailed sensitivity estimates (see, however, the stated references).

The expected DM-induced gamma-ray flux from a direction ψ, averaged over the opening angle $\Delta\psi$ of the detector, is given by

$$\frac{d\Phi_\gamma}{dE_\gamma}(E_\gamma,\psi) = \frac{1}{8\pi}\int_{\Delta_\psi}\frac{d\Omega}{\Delta\psi}\int_{\rm l.o.s}d\ell(\psi)\rho_\chi^2(\mathbf{r}) \times \left(\frac{\langle\sigma v\rangle_{\rm ann}}{m_\chi^2}\sum_f B_f\frac{dN_\gamma^f}{dE_\gamma}\right), \qquad (1)$$

where the integration is performed along the line of sight (l.o.s.), $\langle\sigma v\rangle_{\rm ann}$ is the average velocity-weighted annihilation cross section, m_χ the mass of the DM particle (for which we assume $\chi = \bar{\chi}$), ρ_χ the DM density, B_f the branching ratio into channel f and N_γ^f the number of photons per annihilation. An often quoted reference value for $\langle\sigma v\rangle_{\rm ann}$ is the so-called 'thermal cross section' of $\langle\sigma v\rangle \sim 3\times 10^{-26}{\rm cm}^3{\rm s}^{-1}$, which is the annihilation rate expected for thermally produced WIMPs in the most simple case (i.e. *s*-wave annihilation without resonances or co-annihilations [22]). The right part (in parentheses) of Eq. (1) contains all the particle physics input and, for the typically very small DM velocities, is usually sufficiently independent of $v(\mathbf{r})$ that it can be pulled outside the integrals (note, however, that this is *not*true for strongly velocity-dependent cross-sections like in the case of Sommerfeld enhancement [23,24], resonances or *p*-wave annihilation). It contains the full *spectral*information that we will discuss in some detail in Section 2. The remaining part, sometimes referred to as the astrophysical factor (or '*J*-value', with $J = \int d\Omega \int d\ell,\rho_\chi^2$), contains in that case the full information about the *spatial*distribution of the signal and will be discussed in Section 3.

We continue by reviewing in Section 4 gamma-ray limits on DM annihilation as well as the current status of claimed DM signals. The potentially enormous implications of a signal identification for our understanding of both the underlying particle model and structure formation are then outlined in Section 5, with a focus on the intriguing 130 GeV feature in the direction of the GC. We discuss future prospects for the detection of DM with gamma rays in Section 6 and conclude in Section 7. For most of this review, we will assume that DM consists of WIMPs; many aspects, however, can be applied – or generalized in a straight-forward way – to other cases as well, most notably decaying DM [25] (for which one simply has to replace $\frac{1}{2}\langle\sigma v\rangle\rho_\chi^2 \to m_\chi\Gamma\rho_\chi$ in Eq. (1), where Γ is the decay rate). Where applicable, we will comment on this on the way.

2. Spectral signatures

At tree level, DM particles annihilate into pairs of quarks, leptons, Higgs and weak gauge bosons. The hadronization and further decay of these primary annihilation products leads to the appearance of *secondary photons*, mainly through $\pi^0 \to \gamma\gamma$, and the resulting gamma-ray spectrum dN_γ^f/dE_γ can be obtained from event generators like Pythia [26]. Codes like DarkSUSY [27] provide user-friendly numerical interpolations of these spectra, based on a large number of Pythia runs, but there also exist several analytic parameterizations in the literature [8,28]. Secondary photons show a featureless spectrum with a rather soft cutoff at the kinematical limit $E_\gamma = m_\chi$ and are *universal*in the sense that dN_γ^f/dx (with $x \equiv E_\gamma/m_\chi$) takes a very similar form for almost all channels *f*and only very weakly depends on m_χ. A convincing claim of DM detection based exclusively on this signal, which would show up as a broad bump-like excess over the often rather poorly understood astrophysical background, appears generically rather challenging.

For this reason, it is often much better warranted to focus on the pronounced spectral features that are additionally expected in many DM models – not only because they greatly help to discriminate signals from backgrounds, and hence effectively increase the sensitivity of gamma-ray telescopes to DM signals [29], but also because a detection may reveal a lot about the underlying model for the particle nature of the DM. Before discussing the various types of spectral features in more detail, let us briefly mention further contributions to the total photon yield that do not give rise to such nice spectral features but may still visibly change the spectrum (in particular at $E_\gamma \ll m_\chi$). In models with large branching fractions into e^+e^-pairs, e.g., *inverse Compton*s cattering of those $e^\pm$ on starlight and the cosmic microwave background leads to additional gamma rays [30]. Another source of additional low-energy photons are electroweak [31] and strong [32] radiative corrections, with an additional gauge boson in the final state; these contributions can actually be quite sizable for DM masses much larger than the gauge boson mass, in particular if the tree-level annihilation into a pair of SM particles is suppressed.

2.1. Lines

The direct annihilation of DM pairs into γX– where $X=\gamma, Z, H$or some new neutral state – leads to *monochromatic*gamma rays with $E_\gamma = m_\chi[1 - m_X^2/4m_\chi^2]$, providing a striking signature which is essentially impossible to mimic by astrophysical contributions [33]. Unfortunately, these processes are loop-suppressed with $\mathcal{O}(\alpha_{\rm em}^2)$ and thus usually subdominant, i.e. not actually visible against the continuous (both astrophysical and DM induced) background when taking into account realistic detector resolutions; however, examples of particularly strong line signals exist [24,34]. A space-based detector with resolution $\Delta E/E$= 0.1 (0.01) could, e.g., start to discriminate between $\gamma\gamma$ and γZ lines for DM masses of roughly $m_\chi \lesssim$ 150 GeV ($m_\chi \lesssim$ 400 GeV) if at least one of the lines has a statistical significance of $\gtrsim 5\sigma$[35]. This would, in principle, open the fascinating possibility of doing 'DM spectroscopy' (see also Section 5).

2.2. Internal bremsstrahlung (IB)

Whenever DM annihilates into charged particles, additional final state photons appear at $\mathcal{O}(\alpha_{\rm em})$ that generically dominate the spectrum at high energies. One may distinguish between *final state radiation* (FSR) and *virtual internal bremsstrahlung* (VIB) in a gauge-invariant way [36], where the latter can very loosely be associated to photons radiated from charged virtual particles. FSR is dominated by collinear photons, thus most pronounced for light final state particles, $m_f \ll m_\chi$, and produces a model-independent spectrum with a sharp cut-off at E_γ= m_χ[37,38]; a typical example for a spectrum dominated by these contributions is Kaluza–Klein DM [39]. VIB, on the other hand, dominates if the tree-level annihilation rate is suppressed (like e.g. the annihilation of Majorana particles into light fermions [40]) and/or the final state consists of bosons *and* the *t*-channel particle is almost degenerate with m_χ[41]. It generates pronounced bump-like features at $E_\gamma \lesssim m_\chi$ which closely resemble a slightly distorted line for energy resolutions $\Delta E/E \gtrsim$ 0.1. The exact form of VIB spectra, however, is rather model-dependent [36] – which in principle would allow an efficient discrimination between DM models for large enough statistics (see e.g. [42]).

2.3. Cascade decays

Another possibility to produce pronounced spectral features is DM annihilating into intermediate neutral states, $\chi\chi \to \phi\phi$, which then decay directly ($\phi \to \gamma\gamma$ [43]) or via FSR (e.g. $\phi \to \ell^+\ell^-\gamma$ [44]) into photons. While the latter situation results in a spectrum that resembles the standard FSR case (with a slightly less sharp cut-off and a potentially considerably reduced rate in the degenerate case, $m_\phi \sim m_\ell$), the former process induces a box-shaped spectrum with a width of $\Delta E = \sqrt{m_\chi^2 - m_\phi^2}$; for small mass differences, it is thus indistinguishable from a line.

In Fig. 1, we compare the various different spectra discussed above; in order not to overload this figure, however, we do not include the FSR-dominated spectrum from lepton final states (see e.g. Ref. [39]). Secondary photon spectra from all possible quark or weak gauge boson final states are all contained in the rather thin gray band (we adopted m_χ= 100 GeV, though the result is quite insensitive to this value). For the VIB spectrum, we assumed Majorana DM annihilation into light fermions via a scalar *t*-channel particle ('sfermion') almost degenerate in mass with χ, like encountered in supersymmetry [36], and for the box we chose m_ϕ= 0.95m_χ.

3. Spatial signatures

The peculiar morphology of annihilation signals, tracing directly the DM density, offers another convenient handle for discriminating signals from backgrounds. The most relevant targets are the

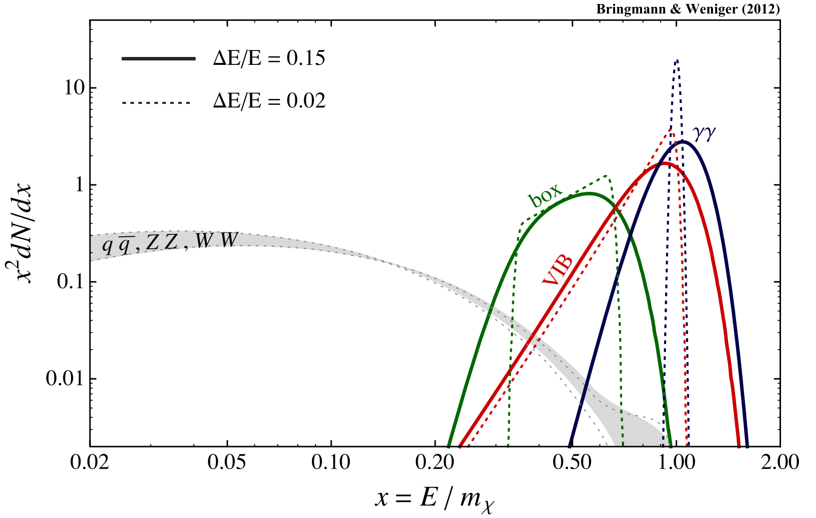

Fig. 1. Various gamma-ray spectra expected from DM annihilation, all normalized to $N(x>0.1) = 1$. Spectra from secondary particles (gray band) are hardly distinguishable. Pronounced peaks near the kinematical endpoint can have different origins, but detectors with very good energy resolutions $\Delta E/E$ may be needed to discriminate amongst them in the (typical) situation of limited statistics. See text for more details about these spectra.

GC, dwarf spheroidal galaxies and galaxy clusters with respective half light radii of roughly $\theta_{1/2} \lesssim 10°$, $\theta_{1/2} \sim 0.1°$ and $\theta_{1/2} \gtrsim 0.1°$. Further important targets are DM clumps or the angular power spectrum of the isotropic gamma-ray background (IGRB), all of which we will discuss in this section.

3.1. Halo profiles and the Galactic center

The arguably brightest source of gamma rays from DM annihilation is the center of our Galaxy. Within a few degrees (say $2° \times 2°$) around the GC, WIMPs would induce a gamma-ray flux of about $\mathcal{O}(10^{-8})$ ph cm^{-2} s^{-1} at the Earth (at > 1 GeV, assuming a thermal annihilation rate into $\bar{b}b$, $m_\chi = 100$ GeV and standard halo profiles), very well in reach of current instruments. However, the line-of-sight to the GC traverses the galactic disc, which harbours numerous high-energetic processes (π^0production in cosmic-ray interactions, Bremsstrahlung and inverse Compton emission, bright point sources); the corresponding gamma-ray fluxes of $\mathcal{O}(10^{-7} - 10^{-6})$ ph cm^{-2}s^{-1} thus outshine DM signals often by orders of magnitude. Furthermore, the uncertainties in the signal and background morphologies make the identification of a DM signal from the inner Galaxy a challenging task.

A useful general parametrization of DM halos, which encompasses a large number of commonly used profiles, reads

$$\rho_\chi^{\alpha\beta\gamma}(r) = \rho_\odot \left[\frac{r}{r_\odot}\right]^{-\gamma} \left[\frac{1 + (r_\odot/r_s)^\alpha}{1 + (r/r_s)^\alpha}\right]^{\frac{\beta-\gamma}{\alpha}}, \tag{2}$$

where r is the distance from the halo center, $r_\odot \simeq 8.5$ kpc the position of the Sun and $\rho_\odot \simeq 0.4$ GeV cm^{-3} the local DM density [45] (see Ref. [46] for a discussion of systematic uncertainties of this quantity and Ref. [47] for a recent study that includes the effect of a slightly oblate DM halo and the possible presence of a dark disc, leading to a normalization which is a factor of ~2–3 larger). The parameters α, β and γ determine the halo shape, and r_s the concentration. The commonly used Navarro–Frenk–White (NFW) profile [48], for example, is obtained for $(\alpha,\beta,\gamma) = (1,3,1)$ (with $r_s \simeq 20$ kpc in case of the Milky Way); the cored isothermal profile follows when setting $(\alpha,\beta,\gamma) = (2,2,0)$ and $r_s \simeq 3.5$ kpc (note, however, that matching observational constraints in principle results in a rather large range of allowed values for r_s [49]). Typically, kinematic observations of line-of-sight velocities do not sufficiently constrain the DM profile, so one has to rely on (extrapolated) results from numerical N-body simulations of dissipationless structure formation in a ΛCDM cosmology [50,51]; see also Refs. [52,53] for a review. Most recent results tend to favor a spherical Einasto profile [54],

$$\rho_\chi^{\text{Einasto}}(r) = \rho_\odot \exp\left(-\frac{2}{\alpha_{\text{E}}} \frac{r^{\alpha_{\text{E}}} - r_\odot^{\alpha_{\text{E}}}}{r_s^{\alpha_{\text{E}}}} \right), \tag{3}$$

over the somewhat steeper NFW profile. Both $r_s$and the halo shape parameter α_E depend on the total halo mass; in case of the Milky Way, numerical simulations yield $\alpha_E \simeq 0.17$ and $r_s \simeq 20$ kpc [50]. Note that for $r \lesssim 0.01 r_s$, there are actually numerical indications for profiles with logarithmic slopes of about $\gamma \sim 1.2$, i.e. steeper than both NFW and Einasto [50,55].

In the Milky Way, baryonic matter dominates the gravitational potential for roughly $r \lesssim r_\odot$, which can have a great impact on the DM distribution with respect to the expectations from DM-only simulations mentioned above. In particular, the cooling and infall of baryons could – by a mechanism known as adiabatic contraction – lead to a steepening of the inner DM profile [56]. However, such a scenario becomes much less likely if, as sometimes found in simulations [57], feedback from star formation and supernovae dominates over cooling and infall processes. In fact, the presence of baryons could have the opposite effect of producing cores rather than cusps, see e.g. the discussion in Refs. [53,58], even for a system with the size of the Milky Way [59] (though such a core might also form only in the very center of a contracted profile [60]). The adiabatic growth of the central supermassive black hole (SMBH) could also generate a central spike of DM within the inner $\sim$10 pc [61] if the SMBH seed starts out close to the GC [62] (SMBH mergers, on the other hand, would rather *destroy*initial cusps in the profile [63]). Microlensing and stellar rotation curve observations can only exclude the most extreme scenarios, yielding upper limits of about $\gamma \lesssim 1.5$ for the logarithmic slope of the DM profile near the GC [64]. The resulting difference in the expected DM annihilation flux from the inner $\sim 0.1^\circ$ around the GC, when comparing the most extreme cases of a cored profile and a profile as steep as this upper limit, amounts to around five orders of magnitude [28]. In any case, the annihilation signal from the GC would most likely appear as an extended source with a peculiar angular profile [65]. Due to the large astrophysical foreground in the very center (e.g. the bright HESS source J1745-290 [66]), the optimal region of interest (ROI) for signal searches extends out to a few degrees and could also lie slightly away from the GC [9,29,67].

A topic that has received only little attention is the possibility that the point of highest DM density could be displaced from the GC. The latter lies at the dynamical center of our Galaxy, coinciding with the position of Sgr A*. Baryons are directly affected by star formation and supernovae, and they shock during galaxy mergers whereas DM does not. It is not unlikely that at least during some periods in the merger and formation history of our Galaxy significant displacements existed [61], like e.g. observed for the SMBH in M87 [68]. If such a displacement remained until today, it could provide a spectacular window into the formation history of our Galaxy, but would also introduce another unknown into the search for a DM signal. Actually, state-of-the-art simulations of late-time spiral galaxies with a significant bar, like the Milky Way, show first hints for such a displacement [60,69].

3.2. Substructure enhancement

For annihilating DM, the gamma-ray emissivity is proportional to the DM density squared. Unresolved substructures in the DM distribution, predicted to exist by all cold DM N-body simulations, can hence potentially have a huge impact on the signal strength [70] – simply because the astrophysical factor in Eq. (1) effectively averages over ρ_χ^2 and one always has $\langle \rho_\chi^2 \rangle > \langle \rho_\chi \rangle^2$ for inhomogeneous distributions. This effect is typically quantified in terms of the so-called boost factor B, which can be defined as the ratio of the actual line-of-sight integral to the one obtained assuming a smooth (e.g. Einasto) component only.

Roughly, every decade in subhalo masses down to the cutoff scale contributes the same to the total gamma-ray flux [71] (with small subhalos possibly being slightly more important [52]), though the details depend crucially on the adopted subhalo mass distribution and concentration, as well as survival probabilities of the smallest clumps (all of which have to be extrapolated over many orders of magnitude from the results of *N*-body simulations). The lower cutoff in the subhalo mass distribution is set by the kinetic decoupling of WIMPs in the early Universe [72] and strongly depends on the DM particle properties [73,74]; while in principle it could be as large as the scale of dwarf galaxies [75], it falls into the range of roughly 10^{-11}–$10^{-3}M_\odot$ for standard MSSM neutralinos [74].

Not too much is known about the precise distribution of substructures, but what one can learn from *N*-body simulations is that due to merger and tidal stripping in the Milky Way halo (see e.g. [51,76] and references therein), fewer substructures are expected in the inner galaxy than in the outer parts (though the surviving subhalos close to the halo center have larger concentrations). This implies that the expected boost factor for GC observations is of order unity [50,76–78], while it may be as large as $\mathcal{O}(1000)$ for galaxy clusters due to the enormous contained hierarchy of masses [77,79,80]. Note also that the expected angular dependence of the signal can change in the presence of large boost factors: in the limit where unresolved substructures completely dominate the total signal, the flux essentially scales with (the line-of-sight integral over) ρ_χ rather than ρ_χ^2; for the Milky Way, this implies that the halo flux emissivity could be changed for $r \gtrsim 1$ kpc [76,81,82].

3.3. Point-like sources

Many complications associated with the GC are avoided when looking at point-like targets outside the galactic disk. The corresponding signals are typically considerably fainter, which is however compensated by the greatly simplified and much smaller astrophysical background.

The probably most promising source class are nearby dwarf spheroidal galaxies. These faint satellites of the Milky Way exhibit the largest known mass-to-light ratios, up to $\sim$1000 $M_\odot/L_\odot$, and do not show signs for gas or recent star formation. As such, they are not expected to be gamma-ray emitters [83]. A canonical set of less than 10 dwarf spheroidals were subject of numerous recent studies [84,85]. Since dwarf spheroidals are DM dominated, stellar kinematics can be efficiently used to constrain the DM content [86,87]. Despite the remaining uncertainties in the shape of the DM profile, it turns out that the integrated signal fluxes are surprisingly robust: the uncertainty is at the level of only 10–50% [88] under the *assumption* of an NFW-like profile in the central part, which is at least naively well motivated (following the idea that such highly DM dominated systems might follow the expectations from CDM only simulations rather closely) and also consistent with observations [89] (but see [90]). However, baryonic processes may still change an initial NFW profile; allowing the inner slope of the density profile to vary between $0 \leq \gamma \leq 1$, e.g., introduces uncertainties corresponding to a factor of a few in the resulting flux, while very steep profiles with $\gamma \geq 1.5$ would increase the flux by an order of magnitude [87]. Significant substructure boosts seem unlikely [87] though it is has been speculated that they might enhance the signal by up to two orders of magnitude in the most optimistic case [91]. This situation is in sharp contrast to the large uncertainties related to the signal flux from the GC that we discussed above and makes dwarf spheroidal galaxies excellent targets to derive robust constraints on the DM annihilation cross-section. Furthermore, it allows a simultaneous analysis of multiple dwarf galaxies, which further increases the sensitivity for DM signals.

Galaxy clusters are the most massive DM dominated virialized objects in the Universe and provide excellent targets to search for an annihilation signal [77,92]. Harboring an enormous hierarchy of substructures, they are the astronomical targets that are expected to maximize the boost factor [80]. In optimistic scenarios [80], they could therefore outshine a signal from local dwarf spheroidals by a factor of a few [88,93], which makes them very attractive as targets for the potential *detection* of a DM signal [77,79,80]. The rather large involved astrophysical uncertainties connected to both the subhalo distribution and cosmic-ray induced gamma rays, on the other hand, imply that robust *limits* derived from cluster observations are usually not competitive. Similar to dwarfs, the sensitivity to cluster signals can be enhanced by a combined analysis [93–95].

Given that they come with no intrinsic astrophysical backgrounds, clumps (subhalos) of DM in the galactic halo that are not massive enough to trigger star formation are further important targets for indirect DM searches [76,96,97]. If discovered as unidentified sources with no counterparts at other wavelengths by surveying instruments like the Fermi-LAT [98], detailed follow-up observations with IACTs could become vital to prove their DM nature by means of additional angular and spectral information.

3.4. Extragalactic diffuse signal and anisotropies

Gamma rays from DM annihilation at cosmological distances, integrated over all redshifts and (sub)halo distributions, appear largely isotropic and add up to the astrophysical IGRB together with contributions from galactic DM annihilation [99–102]. The astrophysical IGRB is presently not very well understood, but believed to stem from unresolved sources like blazars, star-forming galaxies and milli-second pulsars. A WIMP with thermal annihilation cross-section and $\mathcal{O}(100\text{ GeV})$ masses could contribute between $\sim$1% and $\sim$100% to the IGRB, depending on the minimum mass, concentration and abundance of subhalos [103] (though the intrinsic uncertainties related to the substructure distribution may well be even larger [104]). In case of annihilation into $\gamma\gamma$, the signal would be a gamma-ray line broadened by the redshift and provide a peculiar spectral signature to look for in the IGRB [99], which can be efficiently constrained by observations [103].

An interesting approach towards signal identification is also to exploit its angular power spectrum [104–108], which receives contributions from subhalos within our own Galaxy as well as from extragalactic (sub)halos. Let us mention here in particular that anisotropy measurements might turn out to be a feasible way to probe the minimal subhalo mass [106], which would open a completely complementary window into the particle nature of the DM [74].

4. Current status

4.1. Limits

The total number of photons above the detector threshold, typically dominated by secondary photons, is a very convenient and simple measure to constrain possible exotic contributions to observed gamma-ray fluxes. Limits on the DM annihilation rate are therefore usually presented in the $\langle\sigma v\rangle$ vs. m_χ plane, with the assumption of WIMPs dominantly annihilating into $\bar{b}b$ being an often adopted standard that is useful for comparison. Such constraints have been derived from the observation of galaxy clusters [93,94,109–111], external galaxies [28,112,113], globular clusters [114,115], Milky Way satellite dwarf galaxies [85,88,116–121], the GC [122–127] and halo [128,129], or the IGRB [102,103,130,131].

The currently best limits of this kind, for WIMP masses 5 GeV $\lesssim m_\chi \lesssim$ 1 TeV, derive from observations of nearby dwarf galaxies by the Fermi satellite [88][1]; for $m_\chi \lesssim$ 25 GeV, these limits are actually stronger than the 'thermal' rate of $\langle\sigma v\rangle_{b\bar{b}} \sim 3\times10^{-26}\,\text{cm}^3\,\text{s}^{-1}$. At $m_\chi \simeq$ 700 GeV, they weaken to $\langle\sigma v\rangle_{b\bar{b}} \lesssim 4\times10^{-25}\,\text{cm}^3\,\text{s}^{-1}$ and for even higher WIMP masses, the currently strongest limits are presented by the HESS collaboration from observations of the GC region [125]: at $m_\chi \sim$ 1 TeV (10 TeV), those are about a factor of 10 (30) weaker than the thermal value (see also Refs. [117,132] for independent studies of these limits). When comparing limits from different targets, however, one should always keep in mind that the underlying astrophysical uncertainties that enter as the line-of-sight integral in Eq. (1) may be quite different; in particular, as stressed in Section 3, predictions for integrated signal fluxes are much more robust for dwarf galaxies than for the GC.

There have also been various searches for *line signals*: in M31 with HEGRA [133], at the GC with EGRET [134], and with Fermi-LAT GC [135–137] as well as dwarf data [138] and in galaxy clusters [139]. The currently strongest limits presented by the LAT collaboration follow from Fermi observations of the GC region [137] and extend from $\langle\sigma v\rangle_{\gamma\gamma} \lesssim 3\times10^{-29}\text{cm}^3\text{s}^{-1}$ at m_χ= 10 GeV to $\langle\sigma v\rangle_{\gamma\gamma} \lesssim 4\times10^{-27}\text{cm}^3\text{s}^{-1}$ at m_χ= 200 GeV (slightly stronger limits can be found in independent analyses [10,136] for masses from 1 to 300 GeV). Preliminary results from HESS exclude lines above 500 GeV down to cross-sections of $\langle\sigma v\rangle_{\gamma\gamma} \sim 2\times10^{-27}\,\text{cm}^3\,\text{s}^{-1}$ [140]. So far, none of those limits gets close to the expectation for vanilla WIMP models; realistic models featuring particularly strong line signals, however, start to get constrained.

[1] Depending on the assumed profile and small-scale cutoff (as well as subhalo properties), the recently presented constraints from galaxy clusters [111] are nominally even tighter. There are also claims that limits from GC [123,127] or globular cluster [115] observations are actually stronger (though seemingly much less robust) than the dwarf limits.

Table 2
Upper limits at 95%CL (or best-fit value with ±1σ error) on the branching ratios into the secondary line, assuming that the primary line at E_γ=130 GeV is due to annihilation into γX with $X = \gamma$, Z or H. Note that $\langle \sigma v \rangle_{\gamma Z}/\langle \sigma v \rangle_{\gamma\gamma}$ < 2.01 at 95%CL.

γX	m_χ [GeV]	$\langle \sigma v \rangle_{\gamma X}$ [10^{-27} cm^3 s^{-1}]	$\frac{\langle \sigma v \rangle_{\gamma\gamma}}{\langle \sigma v \rangle_{\gamma X}}$	$\frac{\langle \sigma v \rangle_{\gamma Z}}{\langle \sigma v \rangle_{\gamma X}}$	$\frac{\langle \sigma v \rangle_{\gamma H}}{\langle \sigma v \rangle_{\gamma X}}$
$\gamma\gamma$	$129.8 \pm 2.4^{+7}_{-14}$	$1.27 \pm 0.32^{+0.18}_{-0.28}$	1	$0.66^{+0.71}_{-0.48}$	<0.83
γZ	$144.2 \pm 2.2^{+6}_{-12}$	$3.14 \pm 0.79^{+0.40}_{-0.60}$	<0.28	1	<1.08
γH	$155.1 \pm 2.1^{+6}_{-11}$	$3.63 \pm 0.91^{+0.45}_{-0.63}$	<0.17	<0.79	1

The small-scale ($\ell \gtrsim 150$) gamma-ray *anisotropies* observed by Fermi-LAT, indicating the presence of some unresolved source population, can only partially (if at all) be explained by DM annihilation [131]; on the other hand, this can already be used to constrain the distribution of DM subhalos [108]. While some unidentified gamma-ray sources in principle qualify as candidates for annihilating DM *clumps*[141], the presence of any unconventional sources in current gamma-ray data seems very unlikely after taking into account surveys at other wavelengths [98]. Finally, let us mention that the assumed non-observation of gamma-ray point sources from DM annihilation limits the allowed abundance of *ultracompact mini halos* [142], which can be used to put extremely stringent constraints on the power of primordial density perturbations [143].

4.2. Signals

Historically, there have been a couple of claims of potential DM signals in gamma rays. For the GC, e.g., they correspond to DM masses in the ~MeV [144], ~10 GeV [123,145,146], ~100 GeV [147], ~TeV [39,148–150] (sometimes with possible counterparts at radio frequencies [151]) or even multi-TeV range [152]. Possible DM signals in gamma rays have also been claimed in the diffuse gamma-ray flux [153] or from galaxy clusters [154]. While it can be argued that there still remains a bit of controversy in some of these cases, evidence is certainly not compelling; instead, in the past, more refined analyses and new data often tended to either disfavor the DM hypotheses previously put forward or make it less compelling in view of viable alternative, astrophysical explanations [66,111,155–160] (for a discussion of recent DM signal claims not only in gamma rays, see also Ref. [161]). One reason for this is that the claimed signals typically rely on the presence of some broad excess in the differential gamma-ray flux that was mostly attributed to secondary photons which, as stressed before, makes the identification of a DM signal intrinsically error-prone.[2] In this context, it is also worth recalling that neither very small ($m_\chi \ll 100$ GeV) nor very large ($m_\chi \gg 1$ TeV) DM masses are easily accommodated in realistic WIMP frameworks that successfully address shortcomings of the standard model of particle physics. Furthermore, one should appreciate the fact that both CMB [162] and cosmic ray antiproton data [163] provide very stringent constraints on the possibility of $\mathcal{O}(10)$ GeV WIMP DM – even though such a possibility might be interesting from the point of view of direct DM searches [164].

The recently discovered hint for a monochromatic gamma-ray signal at around 130 GeV in the Fermi data of the GC region [9,10], on the other hand, would correspond to a rather natural DM mass of $\mathcal{O}(100)$ GeV and, even more importantly, for the first time provide evidence for a gamma-ray feature which is widely regarded as a *smoking gun signature* for DM [33]. Performing a spectral shape analysis in target regions close to the GC (selected in a data-driven approach by using photons at much lower energies), the signal was found to correspond to a DM mass of $m_\chi = 149 \pm 4^{+8}_{-15}$ GeV for an assumed VIB signal [9] and $m_\chi = 129.8 \pm 2.4^{+7}_{-13}$ GeV for a $\gamma\gamma$ line [10], in each case with a local (global) significance of almost 5σ (more than 3σ). The deduced annihilation rate depends on the DM profile; for an Einasto profile, e.g., it is $\langle \sigma v \rangle_{\ell^+\ell^-\gamma} = (5.2 \pm 1.3^{+0.8}_{-1.2}) \times 10^{-27}$ cm^3 s^{-1} and $\langle \sigma v \rangle_{\gamma\gamma} = (1.27 \pm 0.32^{+0.18}_{-0.28}) \times 10^{-27}$ cm^3 s^{-1}, respectively (see Section 5.2 and Table 2 for a discussion of γZ and γH final states). This excess was confirmed independently [165] by adopting a different statistical technique based on kernel smoothing; this analysis also demonstrated that the intrinsic signal width cannot be much lar-

[2] The only exception is the 511 keV line from e^+e^- annihilation seen by Integral [224]. Its observed non-spherical distribution [157], however, makes a DM interpretation highly unlikely – which in any case would be restricted to a very narrow mass range, $m_e \lesssim m_\chi \lesssim 3$ MeV, in order not to overproduce continuum photons from final state radiation [37,225].

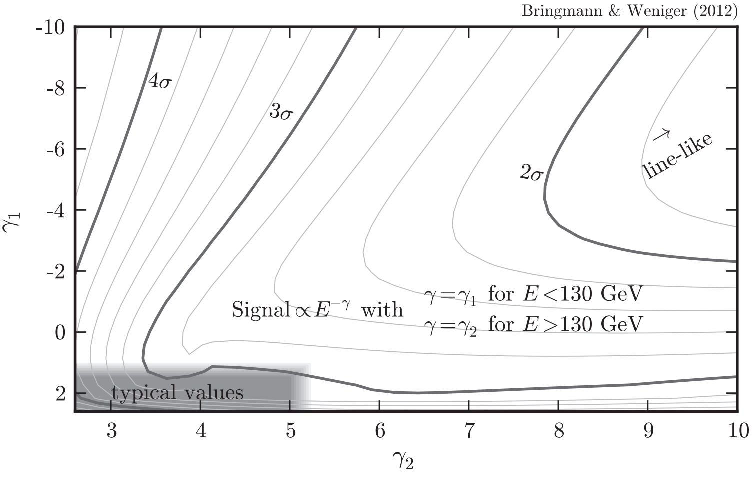

Fig. 2. This plot shows the confidence contours obtained when fitting the 130 GeV signature with a broken power-law with spectral break from γ_1 to γ_2 at 130 GeV (plus the usual background power-law with free normalization and slope). Best fits are obtained for $\Delta\gamma = \gamma_2 - \gamma_1 \gg 10$, when the signal approaches a line-like shape; the gray area indicates parameters that are realistically accessible for astrophysical sources (see e.g. [176]). In light of these results, it is not surprising that also the fit by a hard power-law with superexponential cutoff – as e.g. realized for pulsar emission – plus a power-law background is disfavored w.r.t. a monochromatic line by at least 3σ.

ger than the energy resolution of Fermi LAT ($\sim$10% at 130 GeV) – leaving only a VIB signal, a gamma-ray line or a narrow box as possible explanation in terms of DM annihilation. Later, Su and Finkbeiner [166] adopted a refined spatial template analysis to demonstrate that the existence of a gamma-ray line emitting region of radius $\sim 3°$ (see also Ref. [165]) close to the GC is preferred over the no line hypothesis with a *global* significance of more than 5σ (under the assumption of an Einasto profile).

It is worth emphasizing that the above described signal is the *only* significant line-like feature in the sky that we currently find distinguishable in the data from around 20 GeV to at least 300 GeV (we checked this explicitly by performing line searches along the galactic disc, as well as a subsampling analysis of anti-GC data – see also Refs. [9,10,166]; conflicting claims [165,167] may likely be explained as statistical fluctuations at the expected level). However, it is quite interesting to note that there might be weak evidence for line signals, with much smaller significance but at the same energy, in the direction of galaxy clusters [168]. Further weak evidence for such lines has also been found in some of the unassociated gamma-ray point sources observed by Fermi [169] (but see Ref. [98]). These indications are currently intensely debated [170] – if eventually confirmed with better statistics than currently available, they would significantly strengthen a DM interpretation. Let us also mention that there is no correlation between the Fermi bubbles [150,171] and the line signal at the GC [161,165,166]; the significant overlap [172] of the bubbles with the target regions adopted in Refs. [9,10] is thus purely accidental and related to the peculiar angular distribution of signal and background photons (see also Ref. [173]).

As already stressed, the *intrinsic signal width* is small: assuming a Gaussian instead of a monochromatic signal, we find an upper limit of 18% at 95% CL (though a *pair* of lines might provide a marginally better fit, see Section 5.2). A toy example for an extremely sharp gamma-ray feature with astrophysical origin would e.g. be ICS emission from a hypothetical nearly monochromatic $e^{\pm}$ population at the GC (see e.g. Ref. [174]). Such a population might arise from pile up of electrons during synchrotron cooling, but the resulting ICS gamma-ray spectrum is still disfavoured w.r.t. a monochromatic line by about 3σ. In Fig. 2, we demonstrate furthermore explicitly that a broken power-law, as suggested in Ref. [172], does *not* provide a reasonable fit to the data unless one allows for an absurdly large spectral break $\Delta\gamma \equiv \gamma_2 - \gamma_1 \gg 10$; the best fit is obtained in the line-like limit $\Delta\gamma \to \infty$. As also indicated in the figure, the required spectral indices both above (γ_2) and below (γ_1) the break would in that case be well outside the range of values observed in standard astrophysical sources (the power-law background in our fit, on the other hand, has a spectral index consistent with the expected value of

$\simeq$2.6 [175], mostly determined by cosmic-ray proton collisions with the interstellar medium).[3] Note that a smooth change of γ would make the fit quality even worse, so similar conclusions hold for the more commonly encountered case of a power-law with a super-exponential cutoff, i.e. $dN/dE \propto E^{-\gamma}\exp[-(E/E_{\rm cut})^a]$: for 'typical' values of γ and a (roughly $1 \lesssim \gamma, a \lesssim 2$), but free $E_{\rm cut}$, we find that such a spectrum is always disfavored w.r.t. a monochromatic line by at least 3σ.

Let us now briefly turn to what currently appears as the greatest challenge to a DM interpretation of the observed signal (of course, this necessarily reflects our own bias; for extended discussions see e.g. Refs. [9,10,166,177]; a quite thorough discussion of possible instrumental effects can be found in Ref. [178]). The first caveat is that the signal center seems to be displaced, by about 1.5° or 200 pc, from the dynamical center of the galaxy [166] (see Ref. [165] for an early indication); even if such a displacement might in principle be possible, following our discussion in Section 3.1, this certainly came as a surprise. While the *most likely* center of the emission is clearly displaced by an amount as stated above, on the other hand, the photon distribution still seems to be statistically *consistent*with a single source – with an NFW or Einasto profile – centered exactly at the GC [179] (see also Ref. [180] for a corresponding earlier claim). An even stronger threat to the DM hypothesis might thus be the indication, so far at a weaker level of significance, for a line in part of the gamma rays from cosmic-ray induced air showers in Earth's atmosphere (commonly referred to as Earth limb or Earth albedo) [166,178]. However, the problematic limb photons only appear at a very specific range, $30° \lesssim \theta \lesssim 45°$, of incidence angles (unlike the signal from the GC which shows up at all θ). Furthermore, the majority of events with these incidence angles come actually *not* from the limb but are of astrophysical origin and this larger sample does not show any evidence for a 130 GeV feature [177,178]. This confusing situation might well be an indication that the limb excess is merely a statistical fluctuation that soon will disappear with more limb data.

So far no compelling alternative instrumental [178,181] or astrophysical mechanism has been proposed that could actually produce such a line at 130 GeV (see Ref. [182] for an interesting proof-of-principle with fine-tuned pulsar winds – which however cannot explain the extended morphology of the signal). We stress that all analyses of the line signal so far rely on the publicly available Fermi data and information only, and that line searches operate by construction at the statistical and systematical limitations of the instrument. There has not yet been an official statement from the Fermi collaboration concerning the signal, in particular with respect to whether the energy reconstruction of Pass 7 events is reliable at energies above 100 GeV in light of the recent findings.[4] Eventually, such an independent confirmation of the 130 GeV excess will of course be indispensable.

5. What could we learn from a signal?

Gamma rays may carry important and nontrivial information about the nature of the DM particles. Let us now demonstrate in more detail what kind of information could actually be extracted in case of a signal identification, in particular in case of a sharp spectral signature. For definiteness, we will take the tentative line signal as an *example* and assume in this section that it can indeed be explained by DM.

5.1. Dark matter distribution

A gamma-ray line would allow to study the distribution of DM in the GC with unprecedented accuracy, which could serve as important feedback for state-of-the-art numerical simulations of gravitational clustering. To illustrate this, we show in Fig. 3 the $\pm 1\sigma$ range of the line flux as function of the opening angle θ of a ROI centered on the GC (green band).[5] Obviously, for large galactocentric distances, the flux

[3] To generate the plot, we redid the analysis from Ref. [10] in Reg4 (SOURCE events), replacing the monochromatic line by a broken power-law that changes its spectral index from γ_1 to γ_2 at 130 GeV.

[4] Note that the latest official compilation of Fermi line limits [137] was finalized *before* the first [9] indication for the line signal was announced; it relies on 24 rather than 43 months of data and takes a significantly larger ROI. The tentative signal claim is thus not in tension with those limits [10].

[5] We use here an ROI with hourglass-like shape, defined by $\psi < \min(3°, \theta)$ plus $\psi < \theta$ and $|b/\ell| > 0.7$ (ψ is the angular distance from the GC). Otherwise, we use the same procedure as in Ref. [10] to obtain the line flux, i.e. a power-law + line fit to SOURCE class events.

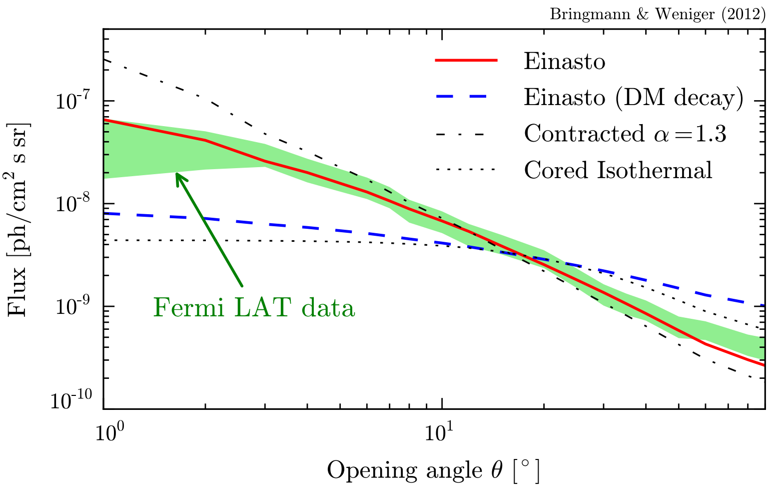

Fig. 3. Comparison of different flux profiles as function of the opening angle θ of an hourglass-shaped ROI that is centered on the GC (see text for detailed definition). In green we show the $\pm 1\sigma$ uncertainty band of the line flux measured inside this region by Fermi LAT after 3.6 years: while compatible with a standard Einasto profile at $\theta \gtrsim 1°$ (as well as an NFW profile; see text), it is incompatible with both a cored and a sufficiently contracted profile, as well as with a signal from DM decay. The green bars indicate which values of θ we actually use in the fits; the profiles are arbitrarily normalized such that they reproduce the correct flux for $\theta = 20°$. Note that we do not make any assumption about a possible displacement of the signal and that the ROI is centered on the GC. (For interpretation of the references to color in this figure legend, the reader is referred to the web version of this article.)

drops because the GC signal is washed out. Remarkably, the flux profile is perfectly consistent with the predictions from a standard Einasto profile (red solid line). The same is true for an NFW profile (not shown), which would in this context only significantly differ closer to the GC, at angles $\theta \lesssim 1°$. The dash-dotted black line shows for comparison the prediction for a DM annihilation signal from a sufficiently contracted profile (chosen to be essentially equivalent, for the angular resolution of Fermi-LAT, to a point source at the GC); at angles $\theta \lesssim 5°$ the measured flux starts to deviate from the predictions, indicating that the 130 GeV signal is not a point source but extended up to these angles. On the other hand, the signal is too concentrated to be compatible with a cored profile (dotted black line, here for a core radius of 3.5 kpc). Note that a contribution from Milky Way subhalos could further boost the signal at angles $\theta \gtrsim 20°$ by a factor of a few [76], which however is not observed and thus might be used to place constraints on subhalo models. DM decay (blue dashed line) would also lead to a flux that is too weak at the GC to be compatible with the observations (unless extreme assumptions on the profile are made [183], which however are likely to be in conflict with microlensing and dynamical constraints [64]).

As already mentioned, there is some evidence for a $\sim$1.5 ° offset of the signal with respect to the GC [166] (though a centered signal might also be consistent with the data [179]). While this observation was certainly unexpected, it might possibly be explained by the interplay between baryons forming a bar and DM [69]. The same bar would however also likely destroy a DM cusp in the center [184]; tidal disruption by the central supermassive black hole may be a further issue to worry about. More data, as well as more detailed simulations along the lines of [60] are thus needed to settle in how far the morphology of the 130 GeV feature is compatible with theoretical expectations. In fact, such an improved understanding could eventually allow to infer important details about the formation history of our Galaxy.

Once the GC signal is established, an exciting future application would be a precise all-sky survey to look for the same 130 GeV feature, aiming at a (partial) map of the Galactic and cosmological DM distribution. For sufficiently large substructure boosts, the 130 GeV feature could for example appear as a bump in the IGRB or in the gamma-ray spectrum of galaxy clusters. So far, no corresponding lines were found in the IGRB [103], which would already put the more optimistic models for substructure evolution from Ref. [107] under some tension if the small-scale cutoff in the subhalo distribution is roughly $10^{-6} M_\odot$ or less (while the reference model used for the Fermi-LAT analysis [103] leads to constraints almost two orders of magnitude weaker than the GC signal strength). On the other hand, there *is*a possible weak indication from galaxy clusters [168]. If confirmed, it would necessarily imply a rather small value for the small-scale cutoff in the subhalo distribution in order to produce the required large boost factors of $\mathcal{O}(10^3)$; this, in turn, could be used to obtain highly complementary bounds on the underlying WIMP model. There is presently no sign for a 130 GeV line in dwarf galaxies and the resulting limits on $(\sigma v)_{\gamma\gamma}$ are about one order of magnitude weaker than what is needed to explain the GC signal [138]; however, these limits are significantly affected by uncertainties in the DM distribution in the dwarfs and in the most favorable case a signal might appear already after a few times larger exposure than currently collected by Fermi-LAT. With more data, it may also be possible to identify a few individual DM subhalos (see e.g. the heavily disputed weak indications for a 130 GeV signal from unidentified sources of the 2FGL [169,170]). The galactic distribution and total number of those subhalos would in principle provide invaluable information on the DM distribution and allow to further discriminate between subhalo models that are currently discussed. Note, however, that presently no precise estimate exists of how many subhalos are actually *expected* to be visible, in the light of results from *N*-body simulations, if the spectrum is dominated by a line; for a secondary spectrum (assuming $\bar{b}b$ annihilation and $m_\chi \simeq 100$ GeV), on the other hand, it was predicted that Fermi should have seen up to a few subhalos [81,97] and the non-observation places a limit on the annihilation cross section comparable to the one obtained from the IGRB [185]. More detailed future studies in this direction would thus certainly be both very interesting and worthwile.

5.2. Dark matter models

At the time of this writing, the literature has already seen a considerable amount of model-building efforts to explain the line signal in terms of *annihilating DM*. This ranges from phenomenological and in some sense model-independent approaches [124,186], or analyses in the context of effective field theories [187–189], to concrete model building. Proposed solutions that mostly fall into the latter category include an additional $U(1)$ symmetry [190], DM as the lightest state of a new scalar multiplet [191], right-handed sneutrino [192] or neutrino [193] DM, axion-mediated DM annihilation [194,195], two-component DM [196], magnetic inelastic DM [197], dipole-interacting DM [198], as well as scalar DM in extensions of the Higgs triplet [199] or Zee–Babu model [200]. Even neutralinos have been proposed as a possible cause of the signal, albeit in non-minimal versions of supersymmetry like no-scale $\mathcal{F}$–$SU(5)$ [201] or the NMSSM [188,194,202] – each time, however, arguing for additional indications in favor of the respective model in collider data. The possibility of *decaying DM* being responsible for the signal has also been entertained [183,203,204] – though the expected angular dependence of the signal in this case is hardly consistent with observations, see the previous subsection.

One generic problem for any realistic model-building is that the annihilation cross section required to fit the data is considerably larger than typically expected for thermally produced DM, at least if the relic density is set by the tree-level annihilation rate. On the particle physics side, possible ways to enhance the annihilation rate in that case include the Sommerfeld enhancement [23,24] in the presence of new light bosonic messenger particles that mediate an attractive force between the initial state DM particles or, at the cost of some fine-tuning, the presence of a resonance (i.e. *s*-channel annihilation via a new neutral particle with $m \simeq 2m_\chi$, the same spin and *CP* properties as the initial state); yet another mechanism might be cascade annihilation [205]. On the astrophysical side, larger annihilation fluxes arise by adopting a larger local DM density for the profile normalization or a profile that is steeper in the innermost part than our reference Einasto profile, Eq. (3); see, however, Fig. 3 for the relatively tight constraints on the latter option. Note that even if one relaxes the theoretically appealing assumption of thermal DM production, one needs to worry about large annihilation rates at tree-level because they would produce secondary photons potentially in stark conflict with continuum gamma-ray data [124,126,139,183,206]; also antiproton [183,207] and radio [207,208] data are quite efficient in constraining such large annihilation rates. This fact can be used to rule out e.g. Wino or Higgsino DM as an explanation for the line (see also below). Antiprotons could be constraining for future experiments not only because of the tree-level annihilation rate, but also due to the associated DM annihilation into *gg*final states if the $\gamma\gamma$ signal is dominated by colored particles in the loop [209].

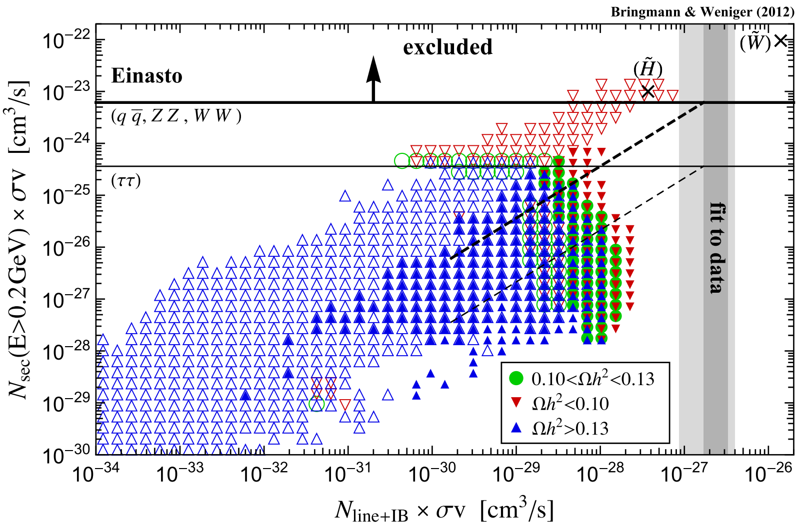

Fig. 4. SUSY scan comparing the expected number of quasi-monochromatic photons (120 GeV $\leq E_\gamma \leq$ 140 GeV) to the number of secondary photons. Green (red, blue) points correspond to models where thermal production leads to a relic density in (smaller than, larger than) the observed range. Filled symbols indicate models where VIB contributes at least 3 times more photons than $\gamma\gamma$ and γZ. Exclusion limits [126] and signal fit (at 1σ and 2σ) both assume an Einasto profile. Dashed lines show the effect of enhancing the annihilation flux by the same amount in both exclusion ($|b|$, $|l| < 5°$) and signal ROI; only models below the dashed line may thus in principle explain the line at 130 GeV. (For interpretation of the references to color in this figure legend, the reader is referred to the web version of this article.)

In order to illustrate the above point, we consider in Fig. 4 the result of a large scan (for details, see Ref. [210]) over the parameter space of the cMSSM and a phenomenological MSSM-7, keeping only neutralino DM models where IB, $\gamma\gamma$ and γZ photons for $E_\gamma \in [120, 140]$ GeV dominate the secondary contribution by a factor of at least 5; for reference, we also show the case of pure Wino ('$\tilde{W}$') and Higgsino ('$\tilde{H}$') DM. Filled symbols correspond to models where IB photons outnumber line photons by at least a factor of 3. Assuming an Einasto profile as in Eq. (3), we also show the required signal strength to account for the line observation (shaded area) as well as limits [126] on the continuum flux from the GC region (solid lines). Note that both limits and signal region are roughly proportional to $\left(\int d\Omega ds\ \rho_\chi^2\right)^{-1}$, albeit integrated over slightly different regions near the GC; assuming this factor to be the same for both regions, dashed lines indicate how limits and signal region would change if adopting a profile that is different from Eq. (3). From this figure, we can draw at least three important conclusions: (i) As already anticipated, the large annihilation rate required to explain the signal cannot easily be achieved for thermally produced neutralino DM. (ii) Even when enhancing the annihilation rate such as to sufficiently increase the production of $\gamma\gamma$ or γZ final states (e.g. by a higher central DM density), it is very difficult to do so without violating the bounds from continuum gamma rays. In fact, the observed correlation between loop- and tree-level rates is generally expected from the optical theorem and should thus not only apply to neutralino DM [207]. (iii) VIB, on the other hand, does not follow this pattern and can thus be argued to be a more natural explanation for such a strong line-like signal – still in need, however, of $\mathcal{O}(10)$ enhancement factors for standard[6] neutralino DM. We note

[6] Let us stress that all supersymmetric models of Fig. 4 assume unification of gauge couplings at the GUT scale, which prohibits a large Wino fraction of the lightest neutralino. Scanning a simple phenomenological MSSM-9 [226], where this assumption is relaxed, we found the top right branch of non-thermally produced models (open red symbols in Fig. 4) to extend all the way to the pure Wino case – albeit always above the (extended) dashed line. However, we could not find any models with larger IB rates than shown in Fig. 4 (possibly due to the restricted nature of the scan and MSSM version employed). Secondary photons from electroweak and strong corrections, see Section 2, were not included and would move the VIB dominated models in Fig. 4 somewhat upwards. While a dedicated future analysis is certainly warranted, let us stress that we still expect the continuum gamma-ray limits to be easily satisfied for VIB dominated, thermally produced neutralinos (antiproton constraints from these channels [227] are likely less stringent [9]).

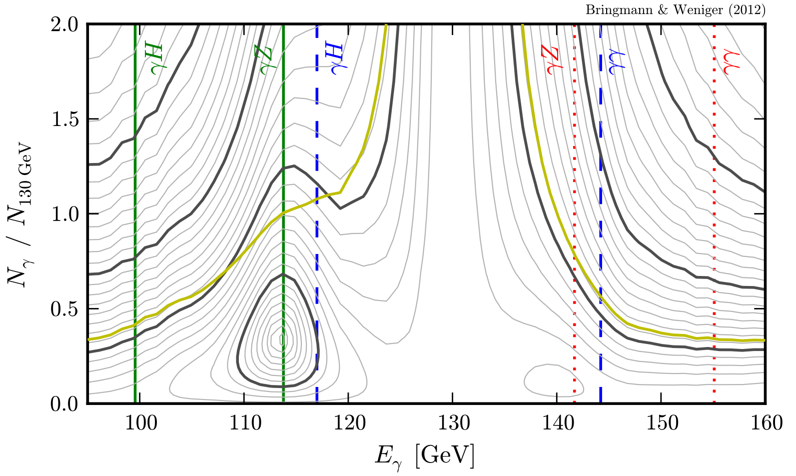

Fig. 5. Significance contour (thick black lines in 1σ steps) and upper limits (yellow line; 95%CL) for a second line. Assuming that the 130 GeV feature is due to $\gamma\gamma$ (green solid), γZ (blue dashed) or γH (red dotted), the vertical lines show the corresponding positions of the other two lines. A very weak hint for a γZ line at 114 GeV can be identified. (For interpretation of the references to color in this figure legend, the reader is referred to the web version of this article.)

that such an enhancement may actually not be unrealistic given the significantly larger values of the local DM density $\rho_\odot$ that are found when assuming a non-spherical DM profile or the presence of a dark disc [47]; furthermore, the most recent simulations of Milky Way like galaxies suggest that baryons should increase the DM density in the central parts by a factor of almost 3, in a way compatible with the angular distribution of the signal as shown in Fig. 3. While most DM model-building so far has focussed on an explanation of the 130 GeV feature in terms of monochromatic gamma-ray lines, also VIB-dominated signals have been considered explicitly in this context [9,193,211].

The possibly only way to avoid the above considerations may be to strongly restrict any coupling of DM to charged standard model particles lighter than m_χ [207]: loop signals could then easily dominate over VIB signals without being in conflict with constraints arising from tree-level annihilations. In such a case, one would rather generically expect not only one but at least two lines [187] and the observed ratio of photon counts (or limits on those) can provide crucial information about the underlying particle model [187,212]. In Fig. 5 we therefore provide significance contours and upper limits for a second line besides the observed 130 GeV feature; for convenience, we summarize these results in Table 2 in terms of limits on the annihilation cross section $(\sigma v)_{\gamma X}$ under the assumption that the signal corresponds to DM annihilation into γY (for $X, Y= \gamma, Z, h$). Interestingly, as observed earlier [166,187], one can see a weak indication (with a significance of around 1.4σ) for a second line at 114 GeV – which coincides surprisingly well with the energy expected for a γZ line if the 130 GeV feature can be attributed to DM annihilation into $\gamma\gamma$; for this case, we also state the best fit value for the ratio of cross sections.

6. Future prospects

6.1. Next decade

The next 10 years will bring a plethora of new results in indirect DM searches. It is right now that experiments start to probe vanilla WIMP DM models and thus will either identify a signal or exclude many of the most common scenarios. Ongoing experiments like Fermi-LAT, HESS-II, VERITAS and MAGIC will continue to take data, may identify new targets for DM searches, profit from a better understanding of astrophysical backgrounds and prepare the stage for planned instruments like CTA or GAMMA-400 with considerably improved characteristics for DM searches. Indirect detection with gamma rays will also profit from an interplay with upcoming results from neutrino searches with IceCube, anti-matter searches with AMS-02, results from the LHC as well as from next-generation direct WIMP detectors. Furthermore, continuously improving results from *N*-body simulations that realistically take into account the various components of baryonic matter will sharpen our understanding of the signal morphology.

Assuming a 10 years lifetime of Fermi-LAT, the limits on the annihilation cross-section that were derived from observations of nearby dwarf galaxies with 2 years of data [88] would improve on purely statistical grounds by a factor of $\sqrt{5}$ to 5, depending on the annihilation channel and the DM mass (which determines whether the limits are derived in the signal-dominated high-energy regime or in the low-energy regime dominated by the diffuse gamma-ray background). Optical surveys like Pan-STARRS, the Dark Energy Survey or the Stromlo Missing Satellite Survey could increase the number of known dwarf spheroidals by a factor of 3, which could additionally increase the constraining power by a factor of $\sqrt{3}$ to 3 in the most optimistic case [213]. Further significant improvements are expected from the upcoming Pass 8 version of the LAT event reconstruction, which will lead to an enhanced effective area for high energy gamma rays, better hadron rejection and an improved energy resolution [214]. It is hence conceivable that Fermi-LAT dwarf limits will improve by a factor up to 10, which could allow to constrain WIMPs with thermal annihilation rate into $\bar{b}b$ up to DM masses of $\sim$600 GeV. Similar improvements might be expected for limits from galaxy clusters [94,109]. DM searches in the GC [126,127,206] and the halo [128], on the other hand, will mostly profit from a refined understanding of astrophysical backgrounds; results from different groups are expected soon. The best limits on annihilation into gamma-ray lines [10] or VIB features [9] are right now based on almost four years of data; more data and improved event reconstruction will strengthen them by at least a factor of $\sqrt{3}$.

By now, HESS observations of the GC provide the strongest limits on DM annihilation with $m_\chi \gtrsim 700$ GeV [125], down to annihilation cross-sections of $\langle\sigma v\rangle_{b\bar{b}} \sim 4 \times 10^{-25}\ \mathrm{cm}^3\ \mathrm{s}^{-1}$. The newly mounted 28 m-diameter telescope HESS-II has an about 3 times lower energy threshold than HESS-I, as well as additional timing information which will improve the rejection of cosmic rays. Both improvements will help to extend the current constraints to lower masses and values of the annihilation cross-section. If Fermi-LAT identifies a DM signal candidate at high enough energies, HESS could quickly confirm it thanks to its large effective area, and provide additional information about the variability and spatial extent of the source. Further results are anticipated from VERITAS, MAGIC and AMS-02 as well. Since VERITAS and MAGIC see the GC at most at angles 33° above horizon (while HESS at angles up to 84°), however, they are mainly interesting for observations of dwarf galaxies and less for DM searches at the GC. Substantial improvement in the TeV regime should eventually come with CTA. Following Ref. [215], observations of the GC are expected to exclude cross-sections down to the thermal one at TeV DM masses, which would be an improvement of up to an order of magnitude with respect to the current HESS constraints (note, however, that this study adopts a factor of about 10 substructure boost of the GC signal w.r.t. what is expected from standard smooth Einasto or NFW profiles). Further improvements with respect to HESS or VERITAS are also expected for dwarf galaxy observations, although they would still hardly be competitive with results from space-based instruments.

Future space-based instruments like GAMMA-400 or CALET/DAMPE will – thanks to an extended imaging calorimeter and a large lever arm to the converter foils – have a much better energy and angular resolution than Fermi LAT. However, they will come with a somewhat smaller effective area. For that reason, DM limits from e.g. dwarf spheroidal observations would likely only be somewhat strengthened in the background limited regime at low energies. On the other hand, these instruments would be excellent machines for detailed follow up studies of DM signal candidates that might be identified in the Fermi-LAT data, in particular in case of pronounced spectral features.

In Fig. 6 we provide a convenient *summary plot* of limits on the DM annihilation cross section into $\bar{b}b$ (in red and blue for space- and ground-based instruments, respectively) as well as in $\gamma\gamma$(in green). The limits are collected as a representative selection of different instruments, and we concentrate on observations of dwarf spheroidal galaxies, the GC and the Galactic halo, since they provide right now the most stringent constraints. All limits are shown as function of the time of their publication, and

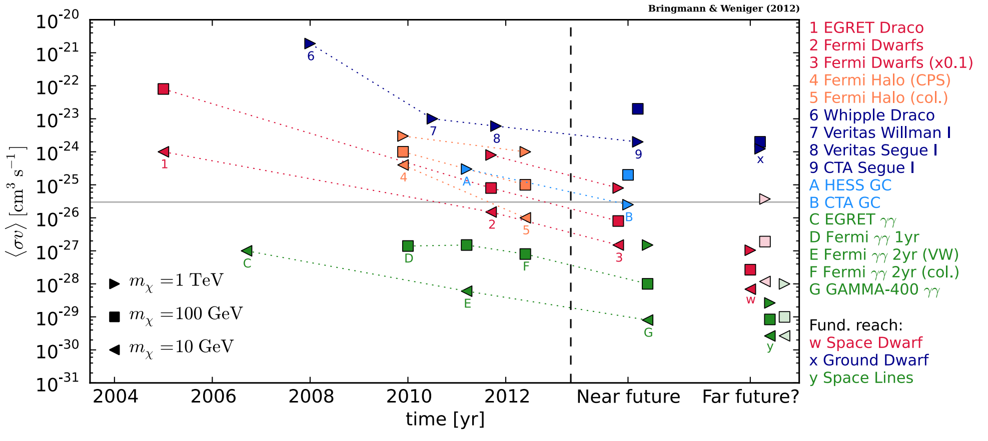

Fig. 6. Time evolution of limits. References: EGRET Draco [216]; Fermi Dwarfs [88]; Fermi Halo (CPS) [101]; Fermi Halo (col.) [129]; Whipple Draco [113]; Veritas Willman I [119]; Veritas Segue I [217]; CTA Segue I and GC [215]; HESS GC [125]; EGRET $\gamma\gamma$ [134]; Fermi $\gamma\gamma$ 1yr [135]; Fermi $\gamma\gamma$ 2yr (VW) [136]; Fermi $\gamma\gamma$ 2yr (col.) [137]; GAMMA-400 [35]. For the dark red, dark green and blue far future 'fundamental' limits, we took only into account systematic limitations (basically assuming that all relevant systematics can be understood at the 1% level); the corresponding observational times can be extremely large in case of space-based telescopes, but are realistic for IACTs. For comparison, the light green and light red symbols show the limits obtained for hypothetical sky exposures about 100 times larger than 10 years Fermi LAT observations in survey mode. (For interpretation of the references to color in this figure legend, the reader is referred to the web version of this article.)

were derived for common assumptions on the DM profile (NFW profiles in most cases; in case of e.g. GC and Galactic halo limits the adopted J-values are mutually consistent within a factor of about two [except for CTA, see above]); the different symbols correspond to limits for DM masses of 10, 100 and 1000 GeV. To the right of the dashed black line, limits expected for the next decade are shown, as well as limits that might be achievable in the more distant future (to be discussed in Section 6.2). In the past eight years, most limits have improved by an order of magnitude; a similar improvement is expected during the upcoming 10 years. Even without excessive boost factors, these limits start to reach deep into the parameter space of WIMP DM models. In particular observations of the GC with Cherenkov telescopes at high energies as well as observations of dwarf spheroidal galaxies with space-based instruments at lower energies have a great potential for deriving constraints or discovering a signal.

Finally, the prospects for a further study of *the 130 GeV feature* in the Fermi-LAT data, if it persists, are extremely good. HESS-II has just seen its first light and given the good performance foreseen for the instrument in hybrid mode, it should allow a quick confirmation of the signal reported in [9,10], if systematic uncertainties are sufficiently under control [35]; for CTA, a mere 50 hrs of data might be enough to confirm the signal [218]. In the case of the future space-based telescopes GAMMA-400 and DAMPE, the improved energy resolution provides an enormous potential not only for the detection of the 130 GeV feature, but also for the efficient discrimination of a VIB feature from one or several lines [15,35]. However, even with GAMMA-400 and its planned excellent energy resolution, the discrimination between a monochromatic line and VIB would require up to a few years of GC observations, whereas the discrimination between one and two lines (in case of $\gamma\gamma$+ γZ final states) could be achievable much faster [35].

A substantial substructure boost will generally be necessary even in the near future to measure the 130 GeV signal elsewhere in the sky, like in dwarf galaxies [138,218], the EGBG [103], galaxy clusters or Milky Way subhalos. On the other hand, the recent claims for an identical signal in galaxy clusters [168] or unidentified sources of the 2FGL [169] are likely to soon be confirmed or refuted in light of the upcoming data and improved telescope performances mentioned above.

6.2. Fundamental reach

Let us finally estimate what may be called the *systematic*or *fundamental* reach of gamma-ray searches for DM signals with current technology. As an instructive exercise, and somewhat complementary to other works (see e.g. Ref. [210]), we will here initially assume infinite observational time or effective area, and concentrate on the remaining systematic limitations. These limitations come from (1) a modeling of astrophysical backgrounds, and (2) the instrument itself (see also Ref. [219] for an instructive comparison of sensitivities of space- and ground-based telescopes).

Numerical codes like GALPROP [220] do an excellent job in modeling the galactic diffuse gamma-ray emission. However, uncertainties related to e.g. the simplified propagation set-up, the interstellar radiation field or models for the gas distribution inhibit *a priori* predictions, and even after performing fits to the data up to $\sim$30% residuals at large and small scales remain [129,175]. At high latitudes, away from the galactic disk, background variations at $\sim 1^\circ$ scales are much less dramatic. Here, we will adopt an optimistic 1% systematic background uncertainty for dwarf galaxy observations.

Relevant instrumental systematics are the spatial and spectral variations in the effective area, incomplete rejection of cosmic rays, and uncertainties in the energy and directional reconstruction (in case of the LAT, e.g., spectral uncertainties in the effective area range from 2% to 10%, depending on signature of interest [221]). We will adopt here an optimistic reference value of 1% as uncertainty for the effective area, which still leaves room for future improvements in the instrumental design. In case of IACTs, we furthermore adopt the aggressive scenario that *all* hadronic showers are rejected, and only the cosmic-ray electron flux remains as an irreducible background (at energies below a few hundred GeV, this approximation is actually already realized with current technology). Such improvement could finally come from an improved imaging of the air shower, and from using a large sensitive array to veto cosmic-ray induced showers by the debris that they typically induce at relatively large angles from the shower axis. Although we do not include this possibility in our estimates, one has to keep in mind that even a rejection of the electron induced background could be finally possible by detecting the Cherenkov light of electrons before their first interaction [222].

We will in the following consider two conceptionally different targets, which are of particular interest for current DM searches: a continuum signal from dwarf spheroidal galaxies and a gamma-ray line signal from the GC.

Dwarf spheroidals. While a combined analysis of several dwarfs could further improve the results, if backgrounds and instrumental systematics are under control, we will here focus on a single prototypic dwarf spheroidal galaxy. We adopt a reference *J*-value of $J \equiv \int d\Omega \int_{\rm l.o.s} d\ell\, \rho_\chi^2 = 10^{19}\ \mathrm{GeV}^2\ \mathrm{cm}^{-5}$ inside an integration cone with radius θ= 0.15°, which is of the expected order for e.g. Draco or Segue I [88,118]. For other values our limits would roughly scale like $\propto J^{-1}$for constant θ, but the potential cuspiness of the DM profile could be used to further strengthen the limits by choosing a smaller integration cone (albeit only for angular resolutions well below 0.1°, see e.g. Fig. 1 in Ref. [84]). In case of space-based instruments, we estimate the level of the diffuse background by the IGRB determined by Fermi [158]. For ground-based instruments, we add on top of that the $e^{\pm}$-flux measured by Fermi-LAT [223].

At the right end of Fig. 6, with dark blue and red markers, we show the limits that result from the requirement that the signal flux from our reference dwarf is below a factor of $2\sqrt{2}\%$ of the background within the integration region θat all energies (corresponding to a 2σ error from 1% instrumental and background systematics). As apparent from this plot, especially space-based instruments still allow a substantial improvement of the limits. To really reach these systematic limitations, however, one would need in case of space-based dwarf galaxy observations (assuming $A_{\rm eff} = 1\ \mathrm{m}^2$) an unrealistic observational time of $10^3(4 \times 10^4, 9 \times 10^5)$ years for DM masses of $m_\chi = 10\ \mathrm{GeV}$ $(100\ \mathrm{GeV}, 1000\ \mathrm{GeV})$, which can only be overcome with a larger effective area. For comparison, we therefore also show by the light red symbols the limits that could be obtained with a hypothetical exposure about 100 times larger than 10 years of Fermi LAT observations in survey mode ($\sim 5 \times 10^{13} \mathrm{cm}^2\mathrm{s}$). Ground based telescopes – which reach much higher event numbers than space based instruments – may reach the quoted 'fundamental' limit already within realistic observational times (e.g. about 100 h for $m_\chi = 1$ TeV and $A_{\rm eff} = 1\ \mathrm{km}^2$). Any improvement beyond these limits would require an efficient rejection of cosmic-ray electrons, which is however extremely challenging (see above).

*Gamma-ray lines.*To estimate the fundamental or systematic limit for gamma-ray line searches in case of space-based instruments, we assume the same ROI and background fluxes as in Ref. [35]; the ROI has a size of $\sim 20^\circ$ and includes the GC. We adopt an energy resolution of 1% (as expected for e.g. GAMMA-400). Requiring that the peak of the line signal after convolution with the instrumental response (assumed to be a Gaussian for simplicity) does not overshoot the background flux by more than $2\sqrt{2}\%$ yields the limits shown by the green markers at the right end of Fig. 6. These fundamental limits are 10–100 times stronger than what is currently obtained with Fermi-LAT (see also Ref. [29] for prospects of observing line or IB features with current and future IACTs). Again, the light green symbols show the limits that would be obtained after a GC exposure 100 times larger than with Fermi LAT after 10 years.

7. Conclusions

In this review, we have argued that one may consider gamma rays as the *golden channel*of indirect searches for DM in view of the extraordinarily rich spectral and angular information they can carry. This does not only help to discriminate signals from backgrounds but could eventually reveal valuable details about the properties of the DM particles. We have discussed the most important signatures in quite some detail and provided an update on current limits, demonstrating that indirect searches start to probe realistic cross sections and thus become competitive probes of physics beyond the standard model.

While too early for a final judgement at the time of this writing, the line feature at 130 GeV that is seen in the Fermi data might turn out to be the most promising DM *signal*claimed so far. In fact, the intrinsic width of this feature must be smaller than roughly 20% (18% at 95%CL) – which leaves lines, VIB or box signals (Fig. 1) as possible channels for an explanation in terms of DM. On the other hand, it is extremely challenging to find any explanation related to astrophysics for such a spectral feature; for example, even a very hard contribution to the gamma-ray flux, with a sharp break at 130 GeV, cannot describe the data in a satisfactory way (Fig. 2). The signal morphology is perfectly consistent with annihilating DM and an Einasto profile for the DM density, at least for distances larger than the possible displacement from the GC by 1–2°, but essentially rules out both cored and more contracted profiles (Fig. 3); decaying DM is also in strong tension with the data. The data show a weak hint for a second peak at 114 GeV (Fig. 5 and Table 2) which is exactly the combination of energies expected for the annihilation of 130 GeV DM particles into $\gamma\gamma$ and γZ final states. However, large annihilation rates into these channels rather generically imply large annihilation rates rate also at tree-level, in potential conflict with continuum gamma-ray limits; VIB, on the other hand, does not suffer from this drawback (Fig. 4).

If confirmed by the Fermi collaboration or other experiments, and in the absence of satisfactory instrumental or astrophysical explanations, this signal would lead to the exciting conclusion that the first particle beyond the standard model has been found in space rather than at a collider. We have discussed at length how astrophysical observations would already now help to determine detailed properties of this new particle. The situation will further improve in the relatively near future given that prospects to study the 130 GeV feature in more detail are extremely good. However, we believe that even if the DM origin of the signal is eventually not confirmed, our analysis serves to make a compelling case for the importance of focussing on clear spectral features in future searches for DM.

During the last 10 years or so, most limits on DM annihilation have improved by about one order of magnitude and this trend is expected to continue for the *next decade* (Fig. 6). We have further estimated the systematics-limited (or 'fundamental') reach of gamma-ray experiments with present technology, demonstrating that there is still quite some room for improvement even beyond those limits expected for the next decade, especially for space-based instruments (but also for ground-based telescopes *if* the cosmic-ray electron background can at least partially be rejected). Eventually, it may thus in principle be possible to probe cross sections down to at least one order of magnitude below the thermal value for TeV-scale particles; for many models, this would correspond to interactions too feeble to show up in any other kind of experiment, including direct or collider searches. While even those limits may not be sufficient to completely close the window for WIMP DM, model-building would certainly need to become increasingly sophisticated to avoid them.

Let us finally stress that in order to fully identify the properties of the DM particles, it will of course be indispensable to correlate a suspected DM signal in gamma rays with results from indirect searches at other wavelengths and with other messengers. The same holds for direct searches and new data from colliders, both of which are guaranteed to deliver substantial new input in the near future – be it in terms of greatly improved limits or actual first hints for a signal. Chances are thus high that the next decade will either bring us a great deal closer to the long-sought nature of DM or, in the most pessimistic scenario in terms of detectional prospects, force us to seriously question the very idea of DM being composed of WIMPs.

Acknowledgments

We warmly thank Lars Bergström, Wilfried Buchmüller, Marco Cirelli, Jan Conrad, Michele Doro, Christian Farnier, Dmitry Gorbunov, Michael Gustafsson, Werner Hofmann, Dieter Horns, Michael Kuhlen, Julien Lavalle, Manfred Lindner, Pat Scott, Thomas Schwetz, Pasquale Serpico, Joe Silk, Peter Tinyakov, Nicola Tomassetti, Nikolay Topchiev and Gabrijela Zaharijas for valuable discussions and feedback on the manuscript. T.B. gratefully acknowledges support from the German Research Foundation (DFG) through the Emmy Noether Grant BR 3954/1-1. T.B. also would like to thank the Institut d'Astrophysique de Paris, and especially Joe Silk, for hospitality during the initial stages of this work. C.W. acknowledges partial support from the European 1231 Union FP7 ITN INVISIBLES (Marie Curie Actions, PITN-GA-2011-289442).

References

[1] M. Roos 2012. Available from: <1208.3662>.
[2] WMAP, E. Komatsu, et al, Astrophys. J. Suppl. 192 (2011) 18. Available from: <1001.4538>.
[3] G. Jungman, M. Kamionkowski, K. Griest, Phys. Rept. 267 (1996) 195. Available from: <hep-ph/9506380>;
L. Bergström, Rept. Prog. Phys. 63 (2000) 793. Available from: <hep-ph/0002126>;
G. Bertone, D. Hooper, J. Silk, Phys. Rept. 405 (2005) 279. Available from: <hep-ph/0404175>.
[4] J.L. Feng, Ann. Rev. Astron. Astrophys. 48 (2010) 495. Available from: <1003.0904>.
[5] G. Bertone, Nature 468 (2010) 389. Available from: <1011.3532>.
[6] A. Czarnecki, W.J. Marciano, Phys. Rev. D64 (2001) 013014. Available from: <hep-ph/0102122>.
[7] P. Bechtle et al, JHEP 1206 (2012) 098. Available from: <1204.4199>.
[8] M. Cirelli et al, JCAP 1103 (2011) 051. Available from: <1012.4515>;
S. Profumo, Ullio P. 2010. Available from: <1001.4086>.;
J. Lavalle, P. Salati 2012. Available from: <1205.1004>.
[9] T. Bringmann et al, JCAP 1207 (2012) 054. Available from: <1203.1312>.
[10] C. Weniger, JCAP 1208 (2012) 007. Available from: <1204.2797>.
[11] M. Tavani et al, Astron. Astrophys. 502 (2009) 995. Available from: <0807.4254>.
[12] VERITAS Collaboration, J. Holder, et al, Astropart. Phys. 25 (2006) 391. Available from: <astro-ph/0604119>.
[13] http://calet.phys.lsu.edu/.
[14] Chang J. Proceedings of the 7th International Workshope "Dark Side of the Universe (DSU 2011)", 2011.
[15] Li Y., Yuan Q. 2012. Available from: <1206.2241>.
[16] http://www.slac.stanford.edu/exp/glast/groups/canda/lat_Performance.htm%relax.
[17] A. Jacholkowska et al, Phys. Rev. D74 (2006) 023518. Available from: <astro-ph/0508349>;
R. Battiston et al, Astropart. Phys. 13 (2000) 51. https://ams02.org/ <astro-ph/9909432>. Available from:.
[18] A. Galper et al., 2012. Available from: <1201.2490>.;
N. Topchiev private communication; Galper A. et al., 2012. Available from: <1210.1457>.
[19] MAGIC Collaboration, J. Aleksic, et al, Astropart. Phys. 35 (2012) 435. Available from: <1108.1477>.
[20] J. Lefaucheur et al., Proceedings of Gamma2012, in press.
[21] CTA Consortium, K. Bernlohr et al., Astropart. Phys., submitted for publication. Available from: <1210.3503>.
[22] K. Griest, D. Seckel, Phys. Rev. D43 (1991) 3191.
[23] A. Sommerfeld, Ann. Phys. 403 (1931) 257;
N. Arkani-Hamed et al, Phys. Rev. D79 (2009) 015014. Available from: <0810.0713>.
[24] J. Hisano, S. Matsumoto, M.M. Nojiri, Phys. Rev. Lett. 92 (2004) 031303. Available from: <hep-ph/0307216>;
J. Hisano et al, Phys. Rev. D71 (2005) 063528. Available from: <hep-ph/0412403>.
[25] W. Buchmuller et al, JHEP 0703 (2007) 037. Available from: <hep-ph/0702184>;
<1205.5283>.
[26] T. Sjöstrand, S. Mrenna, P.Z. Skands, JHEP 0605 (2006) 026. Available from: <hep-ph/0603175>.
[27] P. Gondolo et al, JCAP 0407 (2004) 008. Available from: <astro-ph/0406204>;
Gondolo P. et al., www.darksusy.org.

[28] N. Fornengo, L. Pieri, S. Scopel, Phys. Rev. D70 (2004) 103529. Available from: <hep-ph/0407342>;
J. Cembranos et al, Phys. Rev. D83 (2011) 083507. Available from: <1009.4936>.
[29] T. Bringmann et al, Phys. Rev. D84 (2011) 103525. Available from: <1106.1874>.
[30] E.A. Baltz, L. Wai, Phys. Rev. D70 (2004) 023512. Available from: <astro-ph/0403528>;
M. Regis, P. Ullio, Phys. Rev. D78 (2008) 043505. Available from: <0802.0234>;
J. Zhang et al, Phys. Rev. D80 (2009) 023007. Available from: <0812.0522>.
[31] M. Kachelriess, P. Serpico, Phys. Rev. D76 (2007) 063516. Available from: <0707.0209>;
N.F. Bell et al, Phys. Rev. D78 (2008) 083540. Available from: <0805.3423>;
M. Kachelriess, P. Serpico, M.A. Solberg, Phys. Rev. D80 (2009) 123533. Available from: <0911.0001>;
P. Ciafaloni et al, JCAP 1103 (2011) 019. Available from: <1009.0224>.
[32] M. Asano, T. Bringmann, C. Weniger, Phys. Lett. B709 (2012) 128. Available from: <1112.5158>.
[33] L. Bergström, P. Ullio, J.H. Buckley, Astropart. Phys. 9 (1998) 137. Available from: <astro-ph/9712318>.
[34] M. Gustafsson et al, Phys. Rev. Lett. 99 (2007) 041301. Available from: <astro-ph/0703512>;
E. Dudas et al, JHEP 0908 (2009) 014. Available from: <0904.1745>;
Y. Mambrini, JCAP 0912 (2009) 005. Available from: <0907.2918>;
C. Jackson et al, JCAP 1004 (2010) 004. Available from: <0912.0004>;
C. Arina et al, JCAP 1003 (2010) 024. Available from: <0912.4496>.
[35] L. Bergström et al., 2012. Available from: <1207.6773>.
[36] T. Bringmann, L. Bergström, J. Edsjö, JHEP 01 (2008) 049. Available from: <0710.3169>.
[37] J.F. Beacom, N.F. Bell, G. Bertone, Phys. Rev. Lett. 94 (2005) 171301. Available from: <astro-ph/0409403>.
[38] A. Birkedal et al., 2005. Available from: <hep-ph/0507194>.
[39] L. Bergström et al, Phys. Rev. Lett. 94 (2005) 131301. Available from: <astro-ph/0410359>.
[40] L. Bergström, Phys. Lett. B225 (1989) 372;
R. Flores, K.A. Olive, S. Rudaz, Phys. Lett. B232 (1989) 377.
[41] L. Bergström et al, Phys. Rev. Lett. 95 (2005) 241301. Available from: <hep-ph/0507229>.
[42] M. Perelstein, B. Shakya, JCAP 1010 (2010) 016. Available from: <1007.0018>.
[43] A. Ibarra, Lopez Gehler S., Pato M. 2012. Available from: <1205.0007>.
[44] L. Bergström et al, Phys. Rev. D79 (2009) 081303. Available from: <0812.3895>.
[45] R. Catena, P. Ullio, JCAP 1008 (2010) 004. Available from: <0907.0018>;
P. Salucci et al, Astron. Astrophys. 523 (2010) A83. Available from: <1003.3101>;
P.J. McMillan, MNRAS 414 (2011) 2446. Available from: <1102.4340>;
J. Bovy, S. Tremaine 2012. Available from: <1205.4033>.
[46] M. Pato et al, Phys. Rev. D82 (2010) 023531. Available from: <1006.1322>.
[47] Garbari S. et al., 2012. Available from: <1206.0015>.
[48] J.F. Navarro, C.S. Frenk, S.D.M. White, Astrophys. J. 462 (1996) 563. Available from: <astro-ph/9508025>.
[49] A. Klypin, H. Zhao, R.S. Somerville, Astrophys. J. 573 (2002) 597. Available from: <astro-ph/0110390>;
L.M. Widrow, J. Dubinski, Astrophys. J. 631 (2005) 838. Available from: <astro-ph/0506177>.
[50] J. Diemand et al, Nature 454 (2008) 735. Available from: <0805.1244>.
[51] V. Springel et al, Mon. Not. Roy. Astron. Soc. 391 (2008) 1685. Available from: <0809.0898>.
[52] J. Diemand, B. Moore 2009. Available from: <0906.4340>.
[53] M. Kuhlen, Vogelsberger M., Angulo R. 2012. Available from: <1209.5745>.
[54] J. Einasto, Trudy Inst. Astroz. Alma-Ata 51 (1965) 87.
[55] J. Diemand et al, Mon. Not. Roy. Astron. Soc. 364 (2005) 665. Available from: <astro-ph/0504215>;
J. Stadel et al., 2008. Available from: <0808.2981>.
[56] G.R. Blumenthal et al, Astrophys. J. 301 (1986) 27;
O.Y. Gnedin et al, Astrophys. J. 616 (2004) 16. Available from: <astro-ph/0406247>;
M. Gustafsson, M. Fairbairn, J. Sommer-Larsen, Phys. Rev. D74 (2006) 123522. Available from: <astro-ph/0608634>.
[57] Governato F. et al., 2009. Available from: <0911.2237>.
[58] J.R. Primack, New J. Phys. 11 (2009) 105029. Available from: <0909.2247>;
W. de Blok, Adv. Astron. 2010 (2010) 789293. 0910.3538.
[59] F. Governato et al, Mon. Not. Roy. Astron. Soc. 422 (2012) 1231. Available from: <1202.0554>.
[60] J. Guedes et al, Astrophys. J. 742 (2011) 76. Available from: <1103.6030>.
[61] P. Ullio, H. Zhao, M. Kamionkowski, Phys. Rev. D64 (2001) 043504. Available from: <astro-ph/0101481>.
[62] P. Gondolo, J. Silk, Phys. Rev. Lett. 83 (1999) 1719. Available from: <astro-ph/9906391>.
[63] D. Merritt et al, Phys. Rev. Lett. 88 (2002) 191301. Available from: <astro-ph/0201376>.
[64] F. Iocco et al, JCAP 1111 (2011) 029. Available from: <1107.5810>.
[65] G. Zaharijas, D. Hooper, Phys. Rev. D73 (2006) 103501. Available from: <astro-ph/0603540>;
S. Dodelson, D. Hooper, P.D. Serpico, Phys. Rev. D77 (2008) 063512. Available from: <0711.4621>.
[66] H.E.S.S. Collaboration, F. Aharonian, et al, Phys. Rev. Lett. 97 (2006) 221102. Available from: <astro-ph/0610509>.
[67] P.D. Serpico, G. Zaharijas, Astropart. Phys. 29 (2008) 380. Available from: <0802.3245>.
[68] D. Batcheldor et al, Astrophys. J. 717 (2010) L6. Available from: <1005.2173>.
[69] M. Kuhlen et al., 2012. Available from: <1208.4844>.
[70] J. Silk, A. Stebbins, Astrophys. J. 411 (1993) 439.
[71] J. Diemand, M. Kuhlen, P. Madau, Astrophys. J. 657 (2007) 262. Available from: <astro-ph/0611370>.
[72] A.M. Green, S. Hofmann, D.J. Schwarz, JCAP 0508 (2005) 003. Available from: <astro-ph/0503387>.
[73] S. Profumo, K. Sigurdson, M. Kamionkowski, Phys. Rev. Lett. 97 (2006) 031301. Available from: <astro-ph/0603373>.
[74] T. Bringmann, New J. Phys. 11 (2009) 105027. Available from: <0903.0189>.
[75] L.G.d. Aarssen, T. Bringmann, Pfrommer C. 2012. Available from: <1205.5809>.
[76] L. Pieri et al, Phys. Rev. D83 (2011) 023518. Available from: <0908.0195>.
[77] T.E. Jeltema, J. Kehayias, S. Profumo, Phys. Rev. D80 (2009) 023005. Available from: <0812.0597>.

[78] M. Kamionkowski, S.M. Koushiappas, M. Kuhlen, Phys. Rev. D81 (2010) 043532. Available from: <1001.3144>.
[79] M.A. Sanchez-Conde et al, JCAP 1112 (2011) 011. Available from: <1104.3530>;
L. Gao et al, Mon. Not. Roy. Astron. Soc. 419 (2012) 1721. Available from: <1107.1916>.
[80] A. Pinzke, C. Pfrommer, L. Bergström, Phys. Rev. D84 (2011) 123509. Available from: <1105.3240>.
[81] M. Kuhlen, J. Diemand, P. Madau, Astrophys. J. 686 (2008) 262. Available from: <0805.4416>.
[82] L. Bergstrom et al, Phys. Rev. D59 (1999) 043506. Available from: <astro-ph/9806072>.
[83] E. Baltz et al, Phys. Rev. D61 (2000) 023514. Available from: <astro-ph/9909112>;
C. Tyler, Phys. Rev. D66 (2002) 023509. Available from: <astro-ph/0203242>;
N. Evans, F. Ferrer, S. Sarkar, Phys. Rev. D69 (2004) 123501. Available from: <astro-ph/0311145>.
[84] T. Bringmann, M. Doro, M. Fornasa, JCAP 0901 (2009) 016. Available from: <0809.2269>;
L. Pieri et al, Astron. Astrophys. 496 (2009) 351. Available from: <0812.1494>;
G.D. Martinez et al, JCAP 0906 (2009) 014. Available from: <0902.4715>.
[85] P. Scott et al, JCAP 1001 (2010) 031. Available from: <0909.3300>.
[86] L.E. Strigari et al., 2007. Available from: <0709.1510>.
[87] A. Charbonnier et al., 2011. Available from: <1104.0412>.;
M. Walker et al, Astrophys. J. 733 (2011) L46. Available from: <1104.0411>.
[88] Fermi-LAT, M. Ackermann, et al, Phys. Rev. Lett. 107 (2011) 241302. Available from: <1108.3546>.
[89] L.E. Strigari, C.S. Frenk, S.D. White, Mon. Not. Roy. Astron. Soc. 408 (2010) 2364. Available from: <1003.4268>.
[90] G. Gilmore et al, Astrophys. J. 663 (2007) 948. Available from: <astro-ph/0703308>.
[91] L.E. Strigari et al, Phys. Rev. D75 (2007) 083526. Available from: <astro-ph/0611925>.
[92] S. Colafrancesco, S. Profumo, P. Ullio, Astron. Astrophys. 455 (2006) 21. Available from: <astro-ph/0507575>.
[93] X. Huang, G. Vertongen, C. Weniger, JCAP 1201 (2012) 042. Available from: <1110.1529>.
[94] Fermi-LAT Collaboration, Zimmer S., Conrad J., Pinzke A. 2011. Available from: <1110.6863>.
[95] E. Nezri et al., 2012. Available from: <1203.1165>.;
C. Combet et al, Phys. Rev. D85 (2012) 063517. Available from: <1203.1164>.
[96] G. Lake, Nature 346 (1990) 39.
[97] L. Pieri, G. Bertone, E. Branchini, Mon. Not. Roy. Astron. Soc. 384 (2008) 1627. Available from: <0706.2101>.
[98] H. Zechlin et al, Astron. Astrophys. 538 (2012) A93. Available from: <1111.3514>;
H.S. Zechlin, Horns D. 2012. Available from: <1210.3852>.
[99] L. Bergström, J. Edsjö, P. Ullio, Phys. Rev. Lett. 87 (2001) 251301. Available from: <astro-ph/0105048>.
[100] P. Ullio et al, Phys. Rev. D66 (2002) 123502. Available from: <astro-ph/0207125>;
J.E. Taylor, J. Silk, Mon. Not. Roy. Astron. Soc. 339 (2003) 505. Available from: <astro-ph/0207299>;
S. Blanchet, J. Lavalle 2012. Available from: <1207.2476>.
[101] M. Cirelli, P. Panci, P.D. Serpico, Nucl. Phys. B840 (2010) 284. Available from: <0912.0663>.
[102] K.N. Abazajian, S. Blanchet, J.P. Harding, Phys. Rev. D85 (2012) 043509. Available from: <1011.5090>.
[103] LAT Fermi, A.A. Abdo, et al, JCAP 1004 (2010) 014. Available from: <1002.4415>.
[104] P.D. Serpico et al., 2011. Available from: <1109.0095>.
[105] S. Ando, Phys. Rev. Lett. 94 (2005) 171303. Available from: <astro-ph/0503006>;
S. Ando et al, Mon. Not. Roy. Astron. Soc. 376 (2007) 1635. Available from: <astro-ph/0610155>;
A. Cuoco et al, JCAP 0704 (2007) 013. Available from: <astro-ph/0612559>;
M. Taoso et al, Phys. Rev. D79 (2009) 043521. Available from: <0811.4493>;
J.M. Siegal-Gaskins, JCAP 0810 (2008) 040. Available from: <0807.1328>;
J.M. Siegal-Gaskins, V. Pavlidou, Phys. Rev. Lett. 102 (2009) 241301. Available from: <0901.3776>;
S. Ando, Phys. Rev. D80 (2009) 023520. Available from: <0903.4685>;
A. Ibarra, D. Tran, C. Weniger, Phys. Rev. D81 (2010) 023529. Available from: <0909.3514>;
A. Cuoco et al., 2010. Available from: <1005.0843>.;
J. Zavala et al, Phys. Rev. D83 (2011) 123513. Available from: <1103.0776>.
[106] S. Ando, E. Komatsu, Phys. Rev. D73 (2006) 023521. Available from: <astro-ph/0512217>;
S. Ando et al, Phys. Rev. D75 (2007) 063519. Available from: <astro-ph/0612467>;
M. Fornasa et al, Phys. Rev. D80 (2009) 023518. Available from: <0901.2921>;
S.K. Lee, S. Ando, M. Kamionkowski, JCAP 0907 (2009) 007. Available from: <0810.1284>.
[107] J. Zavala, Springel V., Boylan-Kolchin M. 2009. Available from: <0908.2428>.
[108] M. Fornasa et al., 2012. Available from: <1207.0502>.
[109] LAT Fermi, M. Ackermann, et al, JCAP 1005 (2010) 025. Available from: <1002.2239>;
L. Dugger, T.E. Jeltema, S. Profumo, JCAP 1012 (2010) 015. Available from: <1009.5988>.
[110] S. Ando, D. Nagai, JCAP 1207 (2012) 017. Available from: <1201.0753>.
[111] J. Han et al., 2012. Available from: <1207.6749>.
[112] VERITAS Collaboration, Vassiliev V. et al., (2003) 2679. Available from: <astro-ph/0305584>.;
HEGRA Collaboration, Gotting N. et al., 2003. Available from: <astro-ph/0307334>.;
J. Lavalle et al, Astron. Astrophys. 450 (2006) 1. Available from: <astro-ph/0601298>.
[113] M. Wood et al., 2008. Available from: <0801.1708>.
[114] HESS Collaboration, A. Abramowski, et al, Astrophys. J. 735 (2011) 12. Available from: <1104.2548>.
[115] L. Feng et al, JCAP 1204 (2012) 030. Available from: <1112.2438>.
[116] LAT Fermi, A.A. Abdo, et al, Astrophys. J. 712 (2010) 147. Available from: <1001.4531>;
MAGIC Collaboration, J. Aleksic, et al, JCAP 1106 (2011) 035. Available from: <1103.0477>;
Mazziotta M.N. et al., 2012. Available from: <1203.6731>.
[117] A. Geringer-Sameth, S.M. Koushiappas, Phys. Rev. Lett. 107 (2011) 241303. Available from: <1108.2914>.
[118] I. Cholis, Salucci P. 2012. Available from: <1203.2954>.
[119] VERITAS Collaboration, V. Acciari, et al, Astrophys. J. 720 (2010) 1174. Available from: <1006.5955>.
[120] R. Essig, N. Sehgal, L.E. Strigari, Phys. Rev. D80 (2009) 023506. Available from: <0902.4750>.

[121] R. Essig et al, Phys. Rev. D82 (2010) 123503. Available from: <1007.4199>.
[122] Fermi-LAT Collaboration, Morselli A., Canadas B., Vitale V. 2010. Available from: <1012.2292>.;
R. Crocker et al, Phys. Rev. D81 (2010) 063516. Available from: <1002.0229>.
[123] D. Hooper, T. Linden, Phys. Rev. D84 (2011) 123005. Available from: <1110.0006>.
[124] M.R. Buckley, Hooper D. 2012. Available from: <1205.6811>.
[125] H.E.S.S. Collaboration, A. Abramowski, et al, Phys. Rev. Lett. 106 (2011) 161301. Available from: <1103.3266>.
[126] I. Cholis, Tavakoli M., Ullio P. 2012. Available from: <1207.1468>.
[127] D. Hooper, C. Kelso, Queiroz F.S. 2012. Available from: <1209.3015>.
[128] Fermi-LAT Collaboration, G. Zaharijas, et al, PoS IDM2010 (2011) 111. Available from: <1012.0588>.
[129] LAT Collaboration, Ackermann T.F.M. et al., 2012. Available from: <1205.6474>.
[130] F. Calore, V. De Romeri, F. Donato, Phys. Rev. D85 (2012) 023004. Available from: <1105.4230>.
[131] Fermi LAT Collaboration, M. Ackermann, et al, Phys. Rev. D85 (2012) 083007. Available from: <1202.2856>.
[132] K.N. Abazajian, J.P. Harding, JCAP 1201 (2012) 041. Available from: <1110.6151>.
[133] HEGRA Collaboration, F. Aharonian, et al, Astron. Astrophys. 400 (2003) 153. Available from: <astro-ph/0302347>.
[134] A.R. Pullen, R.R. Chary, M. Kamionkowski, Phys. Rev. D76 (2007) 063006. Available from: <astro-ph/0610295>.
[135] A. Abdo et al, Phys. Rev. Lett. 104 (2010) 091302. Available from: <1001.4836>.
[136] G. Vertongen, C. Weniger, JCAP 1105 (2011) 027. Available from: <1101.2610>.
[137] LAT Collaboration, Ackermann M. et al., 2012. Available from: <1205.2739>.
[138] A. Geringer-Sameth, S.M. Koushiappas 2012. Available from: <1206.0796>.
[139] X.Y. Huang et al., 2012. Available from: <1208.0267>.
[140] C. van Eldik Talk at Gamma 2012, Heidelberg.
[141] A.V. Belikov, Hooper D., Buckley M.R. 2011. Available from: <1111.2613>.;
N. Mirabal et al, Mon. Not. Roy. Astron. Soc. 424 (2012) L64. Available from: <1205.4825>.
[142] M. Ricotti, A. Gould, Astrophys. J. 707 (2009) 979. Available from: <0908.0735>;
P. Scott, S. Sivertsson, S. Sivertsson, Phys. Rev. Lett. 103 (2009) 211301. Available from: <0908.4082>;
B.C. Lacki, J.F. Beacom, Astrophys. J. 720 (2010) L67. Available from: <1003.3466>.
[143] T. Bringmann, P. Scott, Y. Akrami, Phys. Rev. D85 (2012) 125027. Available from: <1110.2484>.
[144] C. Boehm et al, Phys. Rev. Lett. 92 (2004) 101301. Available from: <astro-ph/0309686>;
D. Hooper, L.T. Wang, Phys. Rev. D70 (2004) 063506. Available from: <hep-ph/0402220>;
C. Picciotto, M. Pospelov, Phys. Lett. B605 (2005) 15. Available from: <hep-ph/0402178>.
[145] D. Hooper, L. Goodenough, Phys. Lett. B697 (2011) 412. Available from: <1010.2752>.
[146] K.N. Abazajian, M. Kaplinghat 2012. Available from: <1207.6047>.
[147] A. Cesarini et al, Astropart. Phys. 21 (2004) 267. Available from: <astro-ph/0305075>.
[148] D. Horns, Phys. Lett. B607 (2005) 225. Available from: <astro-ph/0408192>.
[149] T. Lin, D.P. Finkbeiner, G. Dobler, Phys. Rev. D82 (2010) 023518. Available from: <1004.0989>.
[150] G. Dobler, I. Cholis, N. Weiner, Astrophys. J. 741 (2011) 25. Available from: <1102.5095>.
[151] D.P. Finkbeiner, Astrophys. J. 614 (2004) 186. Available from: <astro-ph/0311547>;
D.P. Finkbeiner 2004. Available from: <astro-ph/0409027>.;
G. Dobler, D.P. Finkbeiner, Astrophys. J. 680 (2008) 1222. Available from: <0712.1038>.
[152] S. Profumo, Phys. Rev. D72 (2005) 103521. Available from: <astro-ph/0508628>;
A.V. Belikov, Zaharijas G., Silk J. 2012. Available from: <1207.2412>.;
J. Cembranos, Gammaldi V., Maroto A. 2012. Available from: <1204.0655>.
[153] W. de Boer et al, Astron. Astrophys. 444 (2005) 51. Available from: <astro-ph/0508617>;
G. Hutsi, A. Hektor, M. Raidal, JCAP 1007 (2010) 008. Available from: <1004.2036>.
[154] Han J. et al., 2012. Available from: <1201.1003>.
[155] L. Bergström et al, JCAP 0605 (2006) 006. Available from: <astro-ph/0602632>.
[156] F. Stecker, S. Hunter, D. Kniffen, Astropart. Phys. 29 (2008) 25. Available from: <0705.4311>.
[157] G. Weidenspointner et al, Nature 451 (2008) 159;
A. Boyarsky, D. Malyshev, O. Ruchayskiy, Phys. Lett. B705 (2011) 165. Available from: <1012.5839>.
[158] Fermi-LAT Collaboration, A. Abdo, et al, Phys. Rev. Lett. 104 (2010) 101101. Available from: <1002.3603>.
[159] K.N. Abazajian, JCAP 1103 (2011) 010. Available from: <1011.4275>.
[160] O. Macias-Ramirez et al., 2012. Available from: <1207.6257>.
[161] L. Bergström 2012. Available from: <1205.4882>.
[162] M. Cirelli, F. Iocco, P. Panci, JCAP 0910 (2009) 009. Available from: <0907.0719>;
G. Hutsi et al, Astron. Astrophys. 535 (2011) A26. Available from: <1103.2766>;
S. Galli et al, Phys. Rev. D84 (2011) 027302. Available from: <1106.1528>.
[163] C. Evoli et al, Phys. Rev. D85 (2012) 123511. Available from: <1108.0664>.
[164] DAMA Collaboration, R. Bernabei, et al, Eur. Phys. J. C56 (2008) 333. Available from: <0804.2741>;
CoGeNT Collaboration, C. Aalseth, et al, Phys. Rev. Lett. 106 (2011) 131301. Available from: <1002.4703>;
C. Aalseth et al, Phys. Rev. Lett. 107 (2011) 141301. Available from: <1106.0650>;
G. Angloher et al, Eur. Phys. J. C72 (2012) 1971. Available from: <1109.0702>.
[165] E. Tempel, A. Hektor, M. Raidal 2012. Available from: <1205.1045>.
[166] M. Su, Finkbeiner D.P. 2012. Available from: <1206.1616>.
[167] A. Boyarsky, D. Malyshev, O. Ruchayskiy 2012. Available from: <1205.4700>.
[168] A. Hektor, M. Raidal, E. Tempel 2012. Available from: <1207.4466>.
[169] M. Su, Finkbeiner D.P. 2012. Available from: <1207.7060>.
[170] D. Hooper, T. Linden 2012. Available from: <1208.0828>.;
N. Mirabal 2012. Available from: <1208.1693>.;
A. Hektor, M. Raidal, Tempel E. 2012. Available from: <1208.1996>.
[171] M. Su, T.R. Slatyer, D.P. Finkbeiner, Astrophys. J. 724 (2010) 1044. Available from: <1005.5480>.

[172] S. Profumo, T. Linden, JCAP 1207 (2012) 011. Available from: <1204.6047>.
[173] E. Nezri, J. Lavalle, R. Teyssier 2012. Available from: <1204.4121>.
[174] Weniger C. 2012. Available from: <1210.3013>.
[175] Fermi-LAT Collaboration, Astrophys. J. 750 (2012) 3. Available from: <1202.4039>.
[176] Fermi-LAT Collaboration, Astrophys. J. 710 (2010) 1271. Available from: <1001.4097>.
[177] A. Hektor, M. Raidal, E. Tempel 2012. Available from: <1209.4548>.
[178] D.P. Finkbeiner, Su M., Weniger C. 2012. Available from: <1209.4562>.
[179] K. Rao, D. Whiteson, 2012. Available from: <1210.4934>.
[180] R.Z. Yang et al., 2012. Available from: <1207.1621>.
[181] D. Whiteson 2012. Available from: <1208.3677>.
[182] F. Aharonian, D. Khangulyan, D. Malyshev 2012. Available from: <1207.0458>.
[183] W. Buchmuller, M. Garny 2012. Available from: <1206.7056>.
[184] M.D. Weinberg, N. Katz, Astrophys. J. 580 (2002) 627. Available from: <astro-ph/0110632>.
[185] Fermi LAT Collaboration, M. Ackermann, et al, Astrophys. J. 747 (2012) 121. Available from: <1201.2691>.
[186] S. Tulin, H.B. Yu, K.M. Zurek 2012. Available from: <1208.0009>.
[187] A. Rajaraman, T.M. Tait, D. Whiteson 2012. Available from: <1205.4723>.
[188] Z. Kang et al., 2012. Available from: <1206.2863>.
[189] M.T. Frandsen et al., 2012. Available from: <1207.3971>.
[190] E. Dudas et al., 2012. Available from: <1205.1520>.
[191] J.M. Cline 2012. Available from: <1205.2688>.;
J. Fan, M. Reece 2012. Available from: <1209.1097>.
[192] K.Y. Choi, Seto O. 2012. Available from: <1205.3276>.
[193] L. Bergström 2012. Available from: <1208.6082>.
[194] H.M. Lee, M. Park, W.I. Park 2012. Available from: <1205.4675>.
[195] H.M. Lee, M. Park, W.I. Park 2012. Available from: <1209.1955>.
[196] B.S. Acharya et al., 2012. Available from: <1205.5789>.
[197] N. Weiner, I. Yavin 2012. Available from: <1206.2910>.;
N. Weiner, I. Yavin 2012. Available from: <1209.1093>.
[198] J.H. Heo, C. Kim (2012), 1207.1341.;
J.M. Cline, A.R. Frey, G.D. Moore 2012. Available from: <1208.2685>.
[199] L. Wang, X.F. Han 2012. Available from: <1209.0376>.
[200] S. Baek, P. Ko, E. Senaha 2012. Available from: <1209.1685>.
[201] T. Li et al., 2012. Available from: <1205.3052>.;
T. Li et al., 2012. Available from: <1208.1999>.;
T. Li et al., 2012. Available from: <1210.3011>.
[202] D. Das, U. Ellwanger, Mitropoulos P. 2012. Available from: <1206.2639>.
[203] B. Kyae, J.C. Park 2012. Available from: <1205.4151>.
[204] J.C. Park, S.C. Park 2012. Available from: <1207.4981>.
[205] Y. Bai, Shelton J. 2012. Available from: <1208.4100>.
[206] T. Cohen et al., 2012. Available from: <1207.0800>.
[207] M. Asano et al., 2012, in preparation.
[208] R. Laha et al., 2012. Available from: <1208.5488>.
[209] X. Chu et al., 2012. Available from: <1206.2279>.
[210] L. Bergström, T. Bringmann, J. Edsjö, Phys. Rev. D83 (2011) 045024. Available from: <1011.4514>.
[211] B. Shakya 2012. Available from: <1209.2427>.
[212] I. Oda 2012. Available from: <1207.1537>.
[213] E.J. Tollerud et al, Astrophys. J. 688 (2008) 277. Available from: <0806.4381>;
R. Cotta et al, JCAP 1204 (2012) 016. Available from: <1111.2604>;
H. Jerjen, Adv. Astron. 2010 (2010).
[214] W. Atwood, ASS Meeting 219 (2012) 145.
[215] CTA Collaboration, Doro M. et al., Astrop. Phys., in press. Available from: <1208.5356>.
[216] L. Bergström, D. Hooper, Phys. Rev. D73 (2006) 063510. Available from: <hep-ph/0512317>.
[217] VERITAS Collaboration, Vivier M. 2011. Available from: <1110.6615>.
[218] J. Aleksic, J. Rico, M. Martinez, JCAP 1210 (2012) 032. Available from: <1209.5589>.
[219] S. Funk, Hinton J. 2012. Available from: <1205.0832>.
[220] A.W. Strong, I.V. Moskalenko, Astrophys. J. 509 (1998) 212. Available from: <astro-ph/9807150>.
[221] http://fermi.gsfc.nasa.gov/ssc/data/analysis/LAT_caveats.html.
[222] CTA Consortium, M. Actis, et al, Exper. Astron. 32 (2011) 193. Available from: <1008.3703>.
[223] LAT Fermi, M. Ackermann, et al, Phys. Rev. D82 (2010) 092004. Available from: <1008.3999>.
[224] J. Knodlseder et al, Astron. Astrophys. 441 (2005) 513. Available from: <astro-ph/0506026>.
[225] J.F. Beacom, H. Yuksel, Phys. Rev. Lett. 97 (2006) 071102. Available from: <astro-ph/0512411>.
[226] L. Bergström, T. Bringmann, J. Edsjö, Phys. Rev. D78 (2008) 103520. Available from: <0808.3725>.
[227] M. Garny, A. Ibarra, S. Vogl, JCAP 1204 (2012) 033. Available from: <1112.5155>.